Kinetic study and deactivation phenomena for the methanation of CO_2 and CO mixed syngas on a Ni/Al_2O_3 catalyst

Fabrizio Celoria [a, 1], Fabio Salomone [a, 1, *], Alessio Tauro [a], Marta Gandiglio [b], Domenico Ferrero [b], Isabelle Champon [c], Geneviève Geffraye [c], Raffaele Pirone [a], Samir Bensaid [a]

[a] *Catalytic Reaction Engineering for Sustainable Technologies (CREST) Group, Department of Applied Science and Technology (DISAT), Politecnico di Torino, Corso Duca degli Abruzzi 24, 10129 Torino, Italy.*

[b] *Department of Energy (DENERG), Politecnico di Torino, Corso Duca degli Abruzzi 24, 10129 Torino, Italy.*

[c] U*niversité Grenoble Alpes, CEA LITEN, DTCH, Laboratoire Réacteurs et Procédés (LRP), F-38000, Grenoble, France.*

* *Corresponding author. E-mail address:* fabio.salomone@polito.it

[1] *These authors contributed equally to this work.*

Supplementary Materials

1.	Experimental test bench	2
2.	Test conditions	3
3.	Experimental data processing	5
4.	Gas phase properties	7
5.	Mass and heat transport criteria	13
6.	Derivation of the LHHW kinetic models	16
7.	Characterization of the catalyst	35
8.	Kinetic results	39
9.	Comparisons between model M3 and M4	42
10.	Stability and deactivation results	44
11.	References	47

1. Experimental test bench

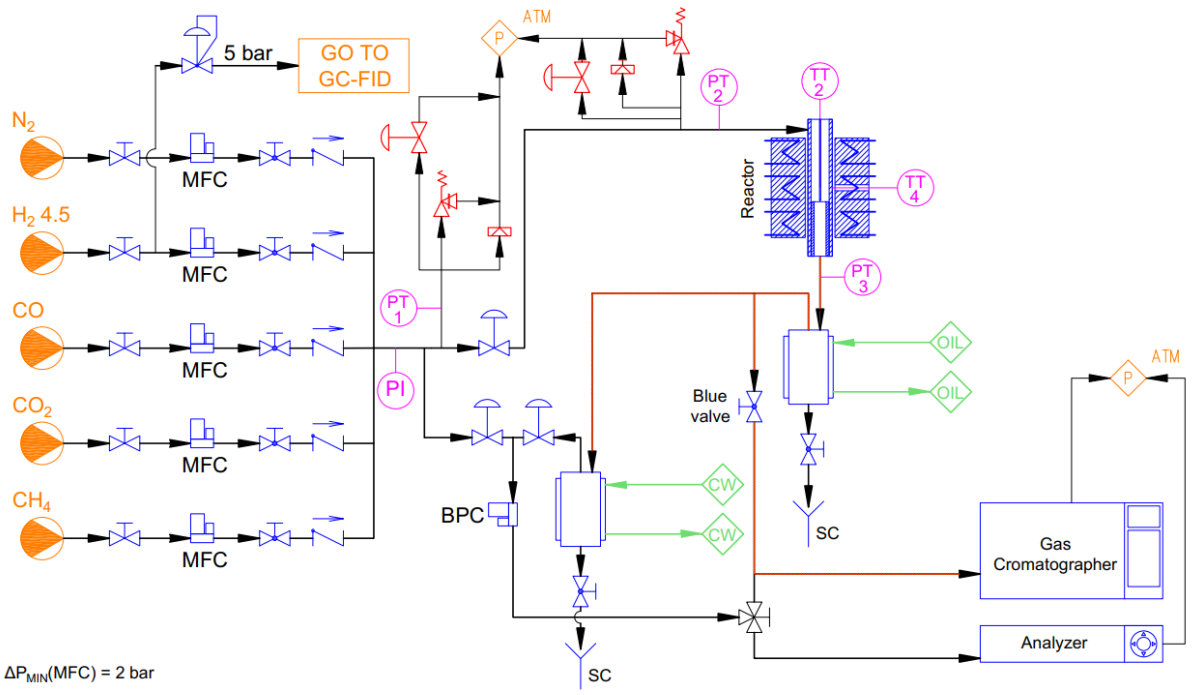

Figure S1. Scheme of the experimental test bench used for the kinetic study and the deactivation tests.

2. Tests conditions

2.1. Kinetic experiments

The 30 different gas mixtures used to perform the kinetic tests are summarized in Table S1, Table S2 and Table S3. All these conditions were performed at two pressures (5 bar and 15 bar) and 6 temperatures (250 °C, 280 °C, 310 °C, 340 °C, 370 °C and 400 °C).

Table S1. Gas composition for the kinetic tests of group I (CO_2 methanation).

Test	Flow rate	H_2	CO_2	CO	CH_4	H_2O	N_2
#	NL/h	vol. %	vol. %	vol. %	vol. %	vol. %	vol. %
T01	60	13.3	6.7	0.0	0.0	0.0	80.0
T02	60	26.7	6.7	0.0	0.0	0.0	66.7
T03	60	53.3	6.7	0.0	0.0	0.0	40.0
T04	60	66.7	6.7	0.0	0.0	0.0	26.7
T05	30	26.7	6.7	0.0	0.0	0.0	66.7
T06	90	26.7	6.7	0.0	0.0	0.0	66.7
T07	60	53.3	13.3	0.0	0.0	0.0	33.3
T08	60	53.3	26.7	0.0	0.0	0.0	20.0
T09	75	32.0	8.0	0.0	8.0	0.0	52.0
T10	75	32.0	8.0	0.0	24.0	0.0	36.0
T11	75	32.0	8.0	0.0	48.0	0.0	12.0

Table S2. Gas composition for the kinetic tests of group II (CO methanation).

Test	Flow rate	H_2	CO_2	CO	CH_4	H_2O	N_2
#	NL/h	vol. %	vol. %	vol. %	vol. %	vol. %	vol. %
T12	90	26.7	0.0	6.7	0.0	0.0	66.7
T13	90	40.0	0.0	6.7	0.0	0.0	53.3
T14	90	53.3	0.0	6.7	0.0	0.0	40.0
T15	60	26.7	0.0	6.7	0.0	0.0	66.7
T16	75	26.7	0.0	6.7	0.0	0.0	66.7
T17	90	40.0	0.0	4.4	0.0	0.0	55.6
T18	90	40.0	0.0	10.0	0.0	0.0	50.0
T19	75	40.0	0.0	5.3	8.0	0.0	46.7
T20	75	40.0	0.0	5.3	16.0	0.0	38.7
T21	75	40.0	0.0	5.3	24.0	0.0	30.7

Table S3. Gas composition for the kinetic tests of group III (CO_2 and CO co-methanation).

Test	Flow rate	H_2	CO_2	CO	CH_4	H_2O	N_2
#	NL/h	vol. %	vol. %	vol. %	vol. %	vol. %	vol. %
T22	90	40.0	3.3	6.7	3.3	0.0	46.7
T23	90	40.0	3.3	1.1	3.3	0.0	52.2
T24	90	40.0	3.3	3.3	10.0	0.0	43.3
T25	90	53.3	3.3	3.3	3.3	0.0	36.7
T26	90	40.0	3.3	3.3	3.3	0.0	50.0
T27	90	26.7	3.3	3.3	3.3	0.0	63.3
T28	90	40.0	3.3	3.3	6.7	0.0	46.7
T29	90	40.0	6.7	3.3	3.3	0.0	46.7
T30	90	40.0	1.1	3.3	3.3	0.0	52.2

2.2. Deactivation experiments

Table S4. Experimental conditions for the stability tests (pressure equal to 5 bar)

Test	Flow rate	H_2	CO_2	CO	C_2H_4	O_2	N_2	Temperature	TOS
#	NL/h	vol. %	vol. %	vol. %	vol. %	vol. %	vol. %	°C	h
S01	60	13.3	3.33	0.0	0.0	0.0	83.4	425	44
S02	60	13.3	3.33	0.0	0.0	0.0	83.4	350	44
S03	60	13.3	3.33	0.0	0.0	0.0	83.4	470	44
S04	60	13.3	0.0	3.33	0.0	0.0	83.4	425	44
S05	60	13.3	0.0	3.33	0.0	0.0	83.4	330	44
S06	60	9.0	0.0	3.0	0.0	0.0	88.0	425	44
S07	60	13.3	1.67	1.67	0.0	0.0	83.3	425	44
S08	60	13.3	1.67	1.67	0.0	0.0	83.3	350	44
S09	60	13.3	3.33	0.0	0.08	0.0	83.4	350	44
S10	60	13.3	3.33	0.0	0.0	0.28	83.4	350	24

3. Experimental data processing

Depending on the type of test, different formulas were used. Experimental values of conversion, yield and selectivity were calculated as final values after a stabilization time. For each kinetic test, the pressure, composition and volumetric flow rate were kept constant, while the temperature was varied in the range 250 – 400 °C. Samples were taken three times after each temperature change, ensuring that the values measured by the TT2 thermocouple (positioned inside the catalytic bed as schematized in Figure S1) reached the set-point value and were stable. In addition, the time taken by the gas mixture leaving the reactor to reach the sampling area was also considered. For the stability tests, however, the temperature was also kept constant, and the sampling of the mixture leaving the reactor was carried out periodically after an initial stabilization time.

3.1. CO_2 methanation (group I)

In the equations, ζ_i is the conversion of the i-th species, σ_i is the selectivity towards the i-th species, η_i is the yield of the i-th species, $\dot{n}_{i,out}$ and $\dot{n}_{i,in}$ (mol/s) are the molar flow rates at the outlet and inlet of the reactor, respectively.

$$\zeta_{CO_2} = \frac{(\dot{n}_{CH_4,out} - \dot{n}_{CH_4,in}) + (\dot{n}_{CO,out} - \dot{n}_{CO,in})}{\dot{n}_{CO_2,in}} \quad (1)$$

$$\sigma_{CH_4} = \frac{\dot{n}_{CH_4,out} - \dot{n}_{CH_4,in}}{\zeta_{CO_2}\dot{n}_{CO_2,in}} \quad (2)$$

$$\sigma_{CO} = \frac{\dot{n}_{CO,out} - \dot{n}_{CO,in}}{\zeta_{CO_2}\dot{n}_{CO_2,in}} \quad (3)$$

$$\eta_{CH_4} = \zeta_{CO_2}\sigma_{CH_4} \quad (4)$$

$$\eta_{CO} = \zeta_{CO_2}\sigma_{CO} \quad (5)$$

3.2. CO methanation (group II)

$$\zeta_{CO} = \frac{(\dot{n}_{CH_4,out} - \dot{n}_{CH_4,in}) + (\dot{n}_{CO_2,out} - \dot{n}_{CO_2,in})}{\dot{n}_{CO,in}} \quad (6)$$

$$\sigma_{CH_4} = \frac{\dot{n}_{CH_4,out} - \dot{n}_{CH_4,in}}{\zeta_{CO}\dot{n}_{CO,in}} \quad (7)$$

$$\sigma_{CO_2} = \frac{\dot{n}_{CO_2,out} - \dot{n}_{CO_2,in}}{\zeta_{CO}\dot{n}_{CO,in}} \quad (8)$$

$$\eta_{CH_4} = \zeta_{CO}\sigma_{CH_4} \quad (9)$$

$$\eta_{CO_2} = \zeta_{CO}\sigma_{CO_2} \quad (10)$$

3.3. CO_2 and CO co-methanation (group III)

$$\zeta_{CO_2} = \frac{\left(\dot{n}_{CO_2,in} - \dot{n}_{CO_2,out}\right)}{\dot{n}_{CO_2,in}} \quad (11)$$

$$\zeta_{CO} = \frac{\left(\dot{n}_{CO,in} - \dot{n}_{CO,out}\right)}{\dot{n}_{CO,in}} \quad (12)$$

$$\zeta_{CO_x} = \frac{\left(\dot{n}_{CO_2,in}\zeta_{CO_2} + \dot{n}_{CO,in}\zeta_{CO}\right)}{\dot{n}_{CO_2,in} + \dot{n}_{CO,in}} \quad (13)$$

$$\eta_{CH_4} = \frac{\dot{n}_{CH_4,out} - \dot{n}_{CH_4,in}}{\dot{n}_{CO_2,in} + \dot{n}_{CO,in}} \quad (14)$$

$$\eta_{CO_2} = \frac{\dot{n}_{CO_2,out} - \dot{n}_{CO_2,in}}{\dot{n}_{CO_2,in} + \dot{n}_{CO,in}} \quad (15)$$

$$\eta_{CO} = \frac{\dot{n}_{CO,out} - \dot{n}_{CO,in}}{\dot{n}_{CO_2,in} + \dot{n}_{CO,in}} \quad (16)$$

$$\sigma_{CH_4} = \frac{\eta_{CH_4}}{\zeta_{CO_x}} \quad (17)$$

$$\sigma_{CO_2} = \frac{\eta_{CO_2}}{\zeta_{CO_x}} \quad (18)$$

$$\sigma_{CO} = \frac{\eta_{CO}}{\zeta_{CO_x}} \quad (19)$$

4. Gas phase properties

4.1. Specific heat capacity and thermodynamic properties

The specific heat capacity and thermodynamic properties were obtained according to the Shomate equation as reported in equations (20) to (22) [1].

$$\tilde{c}_{p,i}^{0}(T) = a_{0,i} + a_{1,i} \cdot \tau + a_{2,i} \cdot \tau^2 + a_{3,i} \cdot \tau^3 + a_{4,i} \cdot \tau^{-2} \quad \text{where} \quad \tau = \frac{T}{1000} \tag{20}$$

$$\Delta\tilde{H}_{T,i}^{0} = \tilde{H}_{T,i}^{0} - \tilde{H}_{298K,i}^{0} = 10^3 \cdot \left(a_{0,i} \cdot \tau + a_{1,i} \cdot \frac{\tau^2}{2} + a_{2,i} \cdot \frac{\tau^3}{3} + a_{3,i} \cdot \frac{\tau^4}{4} - a_{4,i} \cdot \tau^{-1} + a_{5,i} - a_{6,i} \right) \tag{21}$$

$$\tilde{S}_{T,i}^{0} = a_{0,i} \cdot \ln(t) + a_{1,i} \cdot \tau + a_{2,i} \cdot \frac{\tau^2}{2} + a_{3,i} \cdot \frac{\tau^3}{3} - a_{4,i} \cdot \frac{\tau^{-2}}{2} + a_{7,i} \tag{22}$$

In these equations, $\tilde{c}_{p,i}^{0}$ (J/mol/K) is the specific molar heat capacity of the i-th chemical species, $\tilde{H}_{T,i}^{0}$ (J/mol) is its standard enthalpy, $\tilde{S}_{T,i}^{0}$ (J/mol/K) is its standard entropy and T (K) is the absolute temperature. The coefficients $a_{j,i}$ for evaluating the gas phase thermochemistry data for the i-th component are summarized in Table S5.

Table S5. Coefficients for evaluating the gas phase thermochemistry data [1].

	a_0	a_1	a_2	a_3	a_4	a_5	a_6	a_7
CO_2	24.99735	55.18696	-33.69137	7.948387	-0.136638	-403.6075	228.2431	-393.5224
H_2	33.066178	-11.363417	11.432816	-2.772874	-0.158558	-9.980797	172.707974	0
CO	25.56759	6.09613	4.054656	-2.671301	0.131021	-118.0089	227.3665	-110.5271
CH_4	-0.703029	108.4773	-42.52157	5.862788	0.678565	-76.84376	158.7163	-74.8731
H_2O	30.092	6.832514	6.793435	-2.53448	0.082139	-250.881	223.3967	-241.8264
N_2	28.98641	1.853978	-9.647459	16.63537	0.000117	-8.671914	226.4168	0
O_2	31.32234	-20.23531	57.86644	-36.50624	-0.007374	-8.903471	246.7940	0
C	8.527	0	0	0	0	-2.541	16.0633	0

The variation of the enthalpy and entropy of reaction were both evaluated according to the Hess' law as reported in equations (23) and (24). The variation of the Gibbs' free energy of reaction and the equilibrium constant were evaluated according to equation (25).

$$\Delta_r\tilde{H}_{T,\alpha}^{0} = \sum_{i=1}^{N_c} \left(\nu_{i,\alpha} \cdot \Delta_f\tilde{H}_{T,i}^{0} \right) \tag{23}$$

$$\Delta_r\tilde{S}_{T,\alpha}^{0} = \sum_{i=1}^{N_c} \left(\nu_{i,\alpha} \cdot \Delta_f\tilde{S}_{T,i}^{0} \right) \tag{24}$$

$$\Delta_r \tilde{G}^0_{T,\alpha} = \Delta_r \tilde{H}^0_{T,\alpha} - T \cdot \Delta_r \tilde{S}^0_{T,\alpha} = R \cdot T \cdot \ln\left(K_{eq,\alpha}\right) \quad (25)$$

Here, $\Delta_r \tilde{H}^0_{T,\alpha}$ (J/mol), $\Delta_r \tilde{S}^0_{T,\alpha}$ (J/mol/K) and $\Delta_r \tilde{G}^0_{T,\alpha}$ (J/mol) represent the variation of the standard molar enthalpy, entropy and Gibb's free energy of the α-th reaction at the reaction temperature, respectively. $\Delta_f \tilde{H}^0_{T,i}$ (J/mol) and $\Delta_f \tilde{S}^0_{T,i}$ (J/mol/K) represent instead the variation of the standard molar enthalpy and entropy of formation of the i-th species, respectively. $\nu_{i,\alpha}$ is the stoichiometric coefficient (with sign) of the i-th component of the α-th reaction, $K_{eq,\alpha}$ is the equilibrium constant of the α-th reaction, R (8.314 J/mol/K) is the ideal gas constant and N_c is the total number of chemical species.

The specific molar heat capacity of the gas mixture ($\tilde{c}_{p,g}$, J/mol/K) was calculated by means of equation (26), where y_i is the molar fraction of the i-th component.

$$\tilde{c}_{p,g}(T) = \sum_{i=1}^{N_c} \left[y_i \cdot \tilde{c}^0_{p,i}(T) \right] \quad (26)$$

4.2. Dynamic viscosity

The dynamic viscosity of the i-th gas species (μ_i, Pa s) was calculated according to a polynomial interpolation [2] by using equation (27) and the coefficients $b_{j,i}$ for each compound are reported in Table S6.

$$\mu_i(T) = 10^{-7} \cdot \sum_{j=1}^{7} \left(b_{j,i} \cdot \tau^j \right) \quad (27)$$

Table S6. Coefficients for evaluating the dynamic viscosity [3].

	b_0	b_1	b_2	b_3	b_4	b_5	b_6	b_7
CO_2	-20.434	680.07	-432.49	244.22	-85.929	14.45	-0.4564	-20.434
H_2	15.553	299.78	-244.34	249.41	-167.51	62.966	-9.9892	15.553
CO	-4.9137	793.65	875.90	883.75	-572.14	208.42	-32.298	-4.9137
CH_4	-9.9989	529.37	-543.82	548.11	-367.06	140.48	-22.92	-9.9989
H_2O	-6.7541	244.93	419.50	-522.38	348.12	-126.96	19.591	-6.7541
N_2	1.2719	771.45	-809.20	832.47	-553.93	206.15	-32.43	1.2719

The dynamic viscosity of the multicomponent gas mixture (μ_g, Pa s) was evaluated according to the Reichenberg equation (28).

$$\mu_g(T) = \sum_{i=1}^{N_c} K_i \cdot \left\{ 1 + 2 \cdot \sum_{j=1}^{i-1} \left(H_{ij} \cdot K_j \right) + \sum_{j=1 \neq i}^{N_c} \left[\sum_{k=1 \neq i}^{N_c} \left(H_{ij} \cdot H_{ik} \cdot K_j \cdot K_k \right) \right] \right\} \tag{28}$$

In this equation, the coefficients K_i and H_{ij} are defined in equations (29) and (30), respectively.

$$K_i = \frac{y_i \cdot \mu_i}{y_i + \mu_i \cdot \sum_{k=1 \neq i}^{N_c} \left[y_k \cdot H_{ik} \cdot \left(3 + \frac{2 \cdot M_k}{M_i} \right) \right]} \tag{29}$$

$$H_{ij} = \left[\frac{M_i \cdot M_j}{32 \cdot \left(M_i + M_j \right)^3} \right]^{\frac{1}{2}} \cdot \left(B_i \cdot B_j \right)^2 \cdot U_{ij} \tag{30}$$

Here, M (kg/mol) represents the molecular weight, B coefficients are evaluated using equations (31) and (32), while U_{ij} is evaluated with equations (34) and (35). The subscripts i and j represent the i-th and j-th chemical species, respectively.

$$B_i = \frac{(M_i)^{\frac{1}{4}}}{\sqrt{\mu_i \cdot U_i}} \tag{31}$$

$$U_i = \frac{\left[1 + 0.36 \cdot T_{r,i} \cdot \left(T_{r,i} - 1 \right) \right]^{\frac{1}{6}} \cdot F_{R,i}}{\sqrt{T_{r,i}}} \tag{32}$$

$$F_{R,i} = \frac{T_{r,i}^{3.5} + (10 \cdot \mu_{D,r,i})^7}{T_{r,i}^{3.5} \cdot [1 + (10 \cdot \mu_{D,r,i})^7]} \tag{33}$$

$$U_{ij} = \frac{\left[1 + 0.36 \cdot T_{r,ij} \cdot \left(T_{r,ij} - 1 \right) \right]^{\frac{1}{6}} \cdot F_{R,ij}}{\sqrt{T_{r,ij}}} \tag{34}$$

$$F_{R,ij} = \frac{T_{r,ij}^{3.5} + (10 \cdot \mu_{D,r,ij})^7}{T_{r,ij}^{3.5} \cdot [1 + (10 \cdot \mu_{D,r,ij})^7]} \tag{35}$$

Where, T_r is the reduced temperature and $\mu_{D,r}$ is the reduced dipole momentum as reported in equations form (36) to (39). In these equations, T_c (K) is the critical temperature, P_c (Pa) is the critical pressure and μ_D (Debye) is the molecular dipole momentum.

$$T_{r,i} = \frac{T}{T_{c,i}} \tag{36}$$

$$T_{r,ij} = \frac{T}{\sqrt{T_{c,i} \cdot T_{c,j}}} \tag{37}$$

$$\mu_{D,r,i} = 52.46 \cdot \frac{\mu_{D,i}^2 \cdot P_{c,i}}{T_{c,i}^2} \tag{38}$$

$$\mu_{D,r,ij} = \sqrt{\mu_{D,r,i} \cdot \mu_{D,r,j}} \quad (39)$$

In Table S7 are reported the physic-chemical properties of the molecules to calculate the gas mixture properties; σ (m) and ϵ (J) represent respectively the collision diameter and the potential well of the Lennard-Jones potential and k_B ($1.380649 \cdot 10^{-23}$ J/K) is the Boltzmann's constant.

Table S7. Properties of the chemical species [4,5].

	M	T_c	P_c	μ_D	σ	$\frac{\epsilon}{k_B}$
	kg/mol	K	Pa	Debye	m	K
CO_2	$4.40 \cdot 10^{-2}$	304.12	$7.37 \cdot 10^{6}$	0	$4.00 \cdot 10^{-10}$	190
H_2	$2.02 \cdot 10^{-3}$	33.25	$1.30 \cdot 10^{6}$	0	$2.92 \cdot 10^{-10}$	38
CO	$2.80 \cdot 10^{-2}$	132.85	$3.49 \cdot 10^{6}$	0.1	$3.59 \cdot 10^{-10}$	110
CH_4	$1.60 \cdot 10^{-2}$	190.56	$4.60 \cdot 10^{6}$	0	$3.78 \cdot 10^{-10}$	154
H_2O	$1.80 \cdot 10^{-2}$	647.14	$2.21 \cdot 10^{7}$	1.8	$2.73 \cdot 10^{-10}$	356
N_2	$2.80 \cdot 10^{-2}$	126.2	$3.40 \cdot 10^{6}$	0	$3.67 \cdot 10^{-10}$	99.8

4.3. Thermal conductivity

The thermal conductivity of the i-th gas species (λ_i, W/m^2/K) was estimated by means of a polynomial interpolation [2] using equation (40) and the coefficients $c_{j,i}$ for each compound are reported in Table S6.

$$\lambda_i(T) = 10^{-2} \cdot \sum_{j=1}^{6} \left(c_{j,i} \cdot \tau^j\right) \quad (40)$$

Table S8. Coefficients for evaluating the thermal conductivity [3].

	c_0	c_1	c_2	c_3	c_4	c_5	c_6
CO_2	2.8888	-27.018	129.650	-233.290	216.830	-101.120	18.698
H_2	1.5040	62.892	-47.190	47.763	-31.939	11.987	-1.8954
CO	-0.2815	13.999	-23.186	36.018	-30.818	13.379	-2.3224
CH_4	0.4796	1.8732	37.413	-47.440	38.251	-17.283	3.2774
H_2O	2.0103	-7.9139	35.993	-41.390	35.993	-18.974	4.1531
N_2	-0.3216	14.810	-25.473	38.837	-32.133	13.493	-2.2741

The thermal conductivity of the multicomponent gas mixture (λ_g, W/m^2/K) was evaluated according to the Wassiljewa equation (28).

$$\lambda_g = \sum_{i=1}^{N_c} \left[\frac{y_i \cdot \lambda_i}{\sum_{j=1}^{N_c} (y_j \cdot A_{ij})} \right] \tag{41}$$

In this equation, the A_{ij} coefficient is evaluated as reported in equation (42).

$$A_{ij} = \frac{\left[1 + \sqrt{\frac{\mu_i \cdot M_j}{\mu_j \cdot M_i}} \cdot \left(\frac{M_i}{M_j} \right)^{\frac{1}{4}} \right]^2}{\sqrt{8 \left(1 + \frac{M_i}{M_j} \right)}} \tag{42}$$

4.4. Diffusivity

Binary diffusion coefficients were predicted by using the Chapman-Enskog theory [5] as reported is equation (43).

$$\mathcal{D}_{ij} = \frac{3}{8} \cdot \sqrt{\frac{k_B^3 \cdot N_A}{2 \cdot \pi}} \cdot \frac{T^{1.5}}{P \cdot \sigma_{ij}^2 \cdot \Omega_{\mathcal{D},ij}} \cdot \sqrt{\frac{1}{M_i} + \frac{1}{M_j}} \tag{43}$$

Here, $\mathcal{D}_{ij}$ (m^2/s) is the binary diffusion coefficient, N_A ($6.02214076 \cdot 10^{23}$ 1/mol) is the Avogadro's constant, σ_{ij} (m) is the average collision diameter and $\Omega_{\mathcal{D},ij}$ (dimensionless) is the temperature-dependent collision integral for diffusion. The latter parameter was estimated with equation (44) by defining the binary reduced temperature (Θ_{ij}, K) as reported in equation (45) [5].

$$\Omega_{\mathcal{D},ij} = \frac{1.06036}{\Theta_{ij}^{0.15610}} + \frac{0.19300}{\exp(0.47635 \cdot \Theta_{ij})} + \frac{1.03587}{\exp(1.52996 \cdot \Theta_{ij})} + \frac{1.76474}{\exp(3.89411 \cdot \Theta_{ij})} \tag{44}$$

$$\Theta_{ij} = \frac{k_B \cdot T}{\epsilon_{ij}} \tag{45}$$

The average collision diameter and the average binary potential well (ϵ_{ij}, J) are estimated according to the Lorentz-Berthelot combination rule; thus, the pair interactions were evaluated with equations (46) and (47), that are the arithmetic mean and the geometric mean, respectively..

$$\sigma_{ij} = \frac{1}{2} \cdot (\sigma_i + \sigma_j) \tag{46}$$

$$\epsilon_{ij} = \sqrt{\epsilon_i \cdot \epsilon_j} \tag{47}$$

The collision diameter and the potential well are the two parameters that describe the Lennard-Jones potential.

The diffusivity coefficient of a chemical species in a multicomponent gas mixture ($\mathcal{D}_{i,g}$, m^2/s) was estimated by using the Wilke model, that is a simpler model obtained from the Stefan-Maxwell diffusion model. The Wilke correlation is reported in equation (48).

$$\mathcal{D}_{i,g} = \frac{1 - y_i}{\sum_{j \neq i} \left(y_j \cdot \frac{1 - y_i}{\mathcal{D}_{ij}} \right)} \tag{48}$$

In the case of microporous materials, Knudsen diffusion should be considered. Thus, the Knudsen diffusion coefficient of each i-th species ($\mathcal{D}_{i,Kn}$, m^2/s) was evaluated by using equation (49).

$$\mathcal{D}_{i,Kn} = \frac{2}{3} \cdot r_p \cdot \frac{8 \cdot R \cdot T}{\pi \cdot M_i} \tag{49}$$

Here, r_p represents the average pore radius of the catalytic particle. The Knudsen number (Kn) is used to determine the diffusion regime: continuum flow ($Kn < 0.01$), transitional flow ($0.01 < Kn < 10$) and free molecular flow ($Kn > 10$). The Knudsen number can be evaluated by using equation (50).

$$Kn = \frac{\lambda_f}{2 \cdot r_p} = \frac{1}{2 \cdot r_p} \cdot \frac{\mu_g}{P} \cdot \sqrt{\frac{\pi \cdot R \cdot T}{2 \cdot M_g}} \tag{50}$$

Here, λ_f (m) is the mean free path of the molecules, P (Pa) is the pressure and M_g (kg/mol) is the average molecular weight of the gas mixture.

Considering mesoporous materials ($1 < r_p < 25$ nm), transitional flow is generally the predominant diffusion regime. Thus, the effective diffusion coefficient ($\mathcal{D}_{i,e}$, m^2/s) should be estimated by means of a harmonic mean according to the Bosanquet correlation as reported in equation (51).

$$\mathcal{D}_{i,e} = \frac{\varepsilon_p}{\tau_p} \cdot \left(\frac{1}{\mathcal{D}_{i,g}} + \frac{1}{\mathcal{D}_{i,Kn}} \right)^{-1} \tag{51}$$

Here, ε_p is the intraparticle void fraction (porosity) and τ_p is the intraparticle tortuosity.

5. Mass and heat transport criteria

There are four criteria that must be verified to obtain a reliable intrinsic kinetic.

5.1. External mass transport criteria (Mears criterion)

The Mears inequality for inter-particle mass transport is reported in equation (52).

$$\frac{|r_i| \cdot (1-\varepsilon_p) \cdot \rho_s \cdot d_p}{k_{m,i} \cdot C_i} < \frac{0.3}{|n|} \tag{52}$$

In the equation, r_i (mol/kg/s) is the reaction rate of the i-th species, ρ_s (kg/m^3) is the skeletal density of the catalyst, d_p (m) is the particle diameter, $k_{m,i}$ (m/s) is the external mass transfer coefficient of the i-th species, C_i (mol/m^3) is its concentration in the gas mixture and n is the order of the reaction rate.

The external mass transfer coefficients between the bulk of the gas phase and the particle surface are evaluated by evaluating the Sherwood number with equations (53).

$$Sh_i = \frac{k_{m,i} \cdot d_p}{\mathcal{D}_{i,g}} = 2 + 1.1 \cdot Re_p^{0.6} \cdot \sqrt[3]{Sc_i} \tag{53}$$

The particle Reynolds number (Re_p) and the Schmidt number (Sc_i) of the i-th component are evaluated by means of equations (54) and (55), respectively.

$$Re_p = \frac{\rho_g \cdot v_z \cdot d_p}{\mu_g} \tag{54}$$

$$Sc_i = \frac{\mu_g}{\rho_g \cdot \mathcal{D}_{i,g}} \tag{55}$$

5.2. External heat transport criteria (Mears criterion)

The Mears inequality for inter-particle heat transport is reported in equation (56).

$$\frac{(1-\varepsilon_p) \cdot \rho_s \cdot d_p \cdot \sum_{\alpha=1}^{N_r} \left| r_\alpha \cdot \Delta_r \widetilde{H}_{T,\alpha} \right|}{h \cdot T} < \frac{0.3 \cdot R \cdot T}{E_A} \tag{56}$$

In the equation, r_α (mol/kg/s) is the reaction rate of the key component of the α-th reaction and $\Delta_r \widetilde{H}_{T,\alpha}$ (J/mol) is its enthalpy of reaction, h (W/m^2/s) is the external heat transfer coefficient, E_A (J/mol) is the apparent activation energy.

The external heat transfer coefficient between the gas phase and the particle surface is evaluated with the Nusselt number by means of equation (57).

$$Nu = \frac{h \cdot d_p}{\lambda_g} = 2 + 1.1 \cdot Re_p^{0.6} \cdot \sqrt[3]{Pr} \tag{57}$$

The Prandtl number (Pr) is evaluated by means of equation (58).

$$Pr = \frac{\tilde{c}_{p,g} \cdot \mu_g}{M_g \cdot \lambda_g} \tag{58}$$

5.3. Internal mass transport criteria (Weisz-Prater criterion)

The Weisz-Prater inequality for intra-particle mass transport is reported in equation (59).

$$\frac{|r_i| \cdot (1 - \varepsilon_p) \cdot \rho_s \cdot d_p^2}{4 \cdot \mathcal{D}_{i,e} \cdot C_i} < \frac{1}{|n|} \tag{59}$$

In the equation, $\mathcal{D}_{i,e}$ (m/s) is the effective diffusivity coefficient of the i-th species in the multicomponent gas mixture.

5.4. Internal heat transport criteria (Anderson criterion)

The Anderson inequality for intra-particle heat transport is reported in equation (60).

$$\frac{(1 - \varepsilon_p) \cdot \rho_s \cdot d_p \cdot \sum_{\alpha=1}^{N_r} \left| r_\alpha \cdot \Delta_r \tilde{H}_{T,\alpha} \right|}{4 \cdot \lambda_e \cdot T} < \frac{0.75 \cdot R \cdot T}{E_A} \tag{60}$$

In the equation, λ_e (W/m/s) is the effective thermal conductivity, that was estimated by using equation (61).

$$\lambda_e = \lambda_p \cdot (1 - \varepsilon_b) + \lambda_g \cdot \varepsilon_b \tag{61}$$

Here, λ_p (W/m/s) is the thermal conductivity of the particle.

In addition, Table S9 summarizes all the pieces of information for evaluating all the physical properties and the geometry of the reactor.

Table S9. Reactor and catalyst characteristics.

Parameter	Unit	Value	Parameter	Unit	Value
d_p	m	$3 \cdot 10^{-4}$	r_1	m	$2 \cdot 10^{-3}$
L	m	$23 \cdot 10^{-3}$	r_2	m	$3 \cdot 10^{-3}$
ε_b	-	0.4	r_3	m	$5 \cdot 10^{-3}$
λ_p	$W \cdot m^{-1} \cdot K^{-1}$	0.67	r_4	m	$6 \cdot 10^{-3}$
ρ_s	$kg \cdot m^{-3}$	1200	r_p	m	$25 \cdot 10^{-9}$
τ_p	-	2.5	$\hat{c}_{p,s}$	$J \cdot Kg^{-1} \cdot K^{-1}$	1063
ε_p	-	0.6			

6. Derivation of the LHHW kinetic models

6.1. Model M1

Kinetic derivation of the model M1 proposed by Koschany et al. [6]:

Table S10. Reaction steps M1 model

Step	Reactions	Characteristic
(1)	$CO_2(g) + 2* \rightleftarrows CO^* + O^*$	Quasi-equilibrium
(2)	$H_2(g) + 2* \rightleftarrows 2H^*$	Quasi-equilibrium
(3)	$CO^* + H^* \rightleftarrows CHO^* + *$	**RDS**
(4)	$CHO^* + * \rightleftarrows CH^* + O^*$	Low coverage
(5)	$CH^* + 3H^* \rightleftarrows CH_4^* + 3^*$	Low coverage
(6)	$CH_4^* \rightleftarrows CH_4(g) + *$	Low coverage
(7)	$O^* + H^* \rightleftarrows OH^* + *$	Irreversible
(8)	$OH^* + H^* \rightleftarrows H_2O^* + *$	Quasi-equilibrium
(9)	$H_2O^* \rightleftarrows H_2O(g) + *$	Quasi-equilibrium

The formation of the formyl species, elementary step 3, is considered as rate determining step:

$$r = k_3 \Theta_{CO} \Theta_H \tag{62}$$

The coverage of hydrogen is accessible by assuming that dissociative Langmuir adsorption is in quasi-equilibrium:

$$k_2 p_{H_2} \Theta_*^2 = k_{-2} \Theta_H^2 \rightarrow \Theta_H = \sqrt{K_{H_2} p_{H_2}}\, \Theta_* \tag{63}$$

Adsorbed carbon monoxide is formed from dissociative adsorption of carbon dioxide, which is also assumed as Langmuir adsorption in quasi-equilibrium:

$$k_1 p_{CO_2} \Theta_*^2 = k_{-1} \Theta_{CO} \Theta_O \rightarrow \Theta_{CO} = K_{CO_2} p_{CO_2} \frac{\Theta_*^2}{\Theta_O} \tag{64}$$

At steady state, the rate of oxygen hydrogenation must be twice the rate of the rate determining step. It is assumed that reaction equation 7 can also be treated as irreversible.

$$r_7 = 2 \cdot r_3 \tag{65}$$

$$k_7\Theta_O\Theta_H = 2k_3\Theta_{CO}\Theta_H \rightarrow \Theta_O = \frac{2k_3}{k_7}\Theta_{CO} \tag{66}$$

By substituting the oxygen coverage (equation (66)) in equation (64):

$$\Theta_{CO} = \sqrt{\frac{k_7}{2k_3}K_{CO_2}p_{CO_2}}\Theta_* \tag{67}$$

The reaction rate can now be expressed as:

$$r = k_3\sqrt{\frac{k_7}{2k_3}K_{CO_2}p_{CO_2}K_{H_2}p_{H_2}}\Theta_*^2 \tag{68}$$

Assuming hydrogen, carbon monoxide and hydroxyl as most abundant surface intermediates (MASI), the balance over the adsorption sites can be formulated as follows:

$$1 = \Theta_* + \Theta_H\ + \Theta_{CO} + \Theta_{OH} \tag{69}$$

Assuming steps 8 and 9 in equilibrium, the coverage of OH can be expressed as:

$$\frac{K_8}{K_{H_2O}} = \frac{p_{H_2O}\Theta_*^2}{\Theta_H\Theta_{OH}} \tag{70}$$

$$\Theta_{OH} = \frac{K_{H_2O}p_{H_2O}}{K_8\sqrt{K_{H_2}p_{H_2}}}\Theta_* \tag{71}$$

Known these expressions, the fraction of free catalytic sites becomes:

$$\Theta_* = \frac{1}{1 + \sqrt{K_1p_{H_2}} + \sqrt{\frac{k_7}{2k_3}K_{CO_2}p_{CO_2}} + \frac{K_{H_2O}p_{H_2O}}{K_8\sqrt{K_{H_2}p_{H_2}}}} \tag{72}$$

Considering the thermodynamic equilibrium, the reaction rate results in:

$$r_{CH_4} = \frac{k_3\sqrt{\frac{k_7}{2k_3}K_{CO_2}p_{CO_2}K_{H_2}p_{H_2}}\left(1 - \frac{p_{CH_4}p_{H_2O}^2}{p_{CO_2}p_{H_2}^4K_{eq,CO2-meth}}\right)}{\left(1 + \sqrt{K_1p_{H_2}} + \sqrt{\frac{k_7}{2k_3}K_{CO_2}p_{CO_2}} + \frac{K_{H_2O}p_{H_2O}}{K_8\sqrt{K_{H_2}p_{H_2}}}\right)^2} \tag{73}$$

Grouping the constants, the reaction rate is written:

$$r_{CH_4} = \frac{k p_{CO_2}^{0.5} p_{H_2}^{0.5} \left(1 - \frac{p_{CH_4} p_{H_2O}^2}{p_{CO_2} p_{H_2}^4 K_{eq,CO2-meth}}\right)}{\left(1 + \sqrt{K_{H_2} p_{H_2}} + K_{mix} p_{CO_2}^{0.5} + K_{OH} \frac{p_{H_2O}}{p_{H_2}^{0.5}}\right)^2} \quad (74)$$

6.2. Model M2

Kinetic derivation of the model M2 proposed by Quindimil et al. [7]:

Table S11. Reaction steps M2 model

Step	Reactions	Characteristic
(1)	$H_2(g) + 2* \rightleftarrows 2H_2^*$	Quasi-equilibrium
(2)	$CO_2(g) + OH^* \rightleftarrows HCO_3^*$	Quasi-equilibrium
(3)	$HCO_3^* + H^* \rightleftarrows HCOO^* + OH^*$	Quasi-equilibrium
(4)	$HCOO^* + * \rightleftarrows CO^* + OH^*$	**RDS**
(5)	$CO^* \rightleftarrows CO(g) + *$	Quasi-equilibrium
(6)	$CO^* + H^* \rightleftarrows CHO^* + *$	**RDS**
(7)	$CHO^* + * \rightleftarrows CH^* + O^*$	Low coverage
(8)	$CH^* + 3H^* \rightleftarrows CH_4^* + 3^*$	Low coverage
(9)	$CH_4^* \rightleftarrows CH_4(g) + *$	Low coverage
(10)	$O^* + H^* \rightleftarrows OH^* + *$	Low coverage
(11)	$OH^* + H^* \rightleftarrows H_2O^* + *$	Quasi-equilibrium
(12)	$H_2O^* \rightleftarrows H_2O(g) + *$	Low coverage

The CO_2 disappearance rate is equal to the rate of elementary step 4

$$-r_{CO_2} = r_4 = k_4 \Theta_{HCOO} \Theta_* \tag{75}$$

Considering that Langmuir H_2 adsorption (step 1) is in quasi-equilibrium, the H_2 coverage can be expressed as:

$$k_1 p_{H_2} \Theta_*^2 = k_{-1} \Theta_H \rightarrow \Theta_H = \sqrt{\frac{k_1}{k_{-1}} p_{H_2} \Theta_*^2} = \sqrt{K_1 p_{H_2}} \Theta_* \tag{76}$$

Elementary steps 2 and 3 are also in quasi-equilibrium:

$$k_2 p_{CO_2} \Theta_{OH} = k_{-2} \Theta_{HCO_3} \rightarrow \Theta_{HCO_3} = \frac{k_2}{k_{-2}} p_{CO_2} \Theta_{OH} = K_2 p_{CO_2} \Theta_{OH} \tag{77}$$

$$k_3 \Theta_{HCO_3} \Theta_H = k_{-3} \Theta_{HCOO} \Theta_{OH} \rightarrow \Theta_{HCOO} = \frac{k_3}{k_{-3}} \frac{\Theta_{HCO_3} \Theta_H}{\Theta_{OH}} = K_3 \frac{\Theta_{HCO_3} \Theta_H}{\Theta_{OH}} \tag{78}$$

By substituting the expression (76) and (77) into the equation (78):

$$\Theta_{HCOO} = K_2 K_3 p_{CO_2} \sqrt{K_1 p_{H_2}} \Theta_* \tag{79}$$

Then, replacing formate coverage in equation (75), the rate equation can be formulated as:

$$-r_{CO_2} = k_4 K_2 K_3 p_{CO_2} \sqrt{K_1 p_{H_2}} \Theta_*^2 \tag{80}$$

Assuming that hydrogen dissociated atoms, formates, carbonyls and hydroxyls occupy most of the active sites, the active sites balance is expressed as:

$$1 = \Theta_* + \Theta_H + \Theta_{HCOO} + \Theta_{CO} + \Theta_{OH} \tag{81}$$

Elementary step 5 is in quasi-equilibrium:

$$k_5 \Theta_{CO} = k_{-5} p_{CO} \Theta_* \rightarrow \Theta_{CO} = \frac{k_{-5}}{k_5} p_{CO} \Theta_* = \frac{p_{CO}}{K_5} \Theta_* \tag{82}$$

Θ_{OH} is derived assuming step 11 in quasi-equilibrium and low H_2O coverage in step 12:

$$k_{11} \Theta_{OH} \Theta_H = k_{-11} \Theta_{H_2O} \Theta_* \rightarrow \Theta_{OH} = \frac{k_{-11}}{k_{11}} \frac{\Theta_{H_2O} \Theta_*}{\Theta_H} = \frac{\Theta_{H_2O}}{K_{11} \sqrt{K_1 p_{H_2}}} \tag{83}$$

$$k_{12} \Theta_{H_2O} = k_{-12} p_{H_2O} \rightarrow \Theta_{H_2O} = \frac{k_{-12}}{k_{12}} p_{H_2O} \Theta_* = \frac{p_{H_2O}}{K_{12}} \Theta_* \tag{84}$$

Then, the hydroxyl coverage is defined as:

$$\Theta_{OH} = \frac{p_{H_2O} \Theta_*}{K_{11} K_{12} \sqrt{K_1 p_{H_2}}} \tag{85}$$

Introducing equations (82), (83), (84) and (85) in equation (81), the fraction of free active sites can be formulated as follows as function of known variables:

$$1 = \Theta_* + \sqrt{K_1 p_{H_2}} \Theta_* + K_2 K_3 p_{CO_2} \sqrt{K_1 p_{H_2}} \Theta_* + \frac{p_{CO}}{K_5} \Theta_* + \frac{p_{H_2O} \Theta_*}{K_{11} K_{12} \sqrt{K_1 p_{H_2}}} \tag{86}$$

$$\Theta_* = \frac{1}{1 + \sqrt{K_1 p_{H_2}} + K_2 K_3 p_{CO_2} \sqrt{K_1 p_{H_2}} + \frac{p_{CO}}{K_5} + \frac{p_{H_2O}}{K_{11} K_{12} \sqrt{K_1 p_{H_2}}}} \tag{87}$$

Considering thermodynamic equilibrium, the Reverse Water Gas Shift reaction becomes:

$$-r_{CO_2} = \frac{k_4 K_2 K_3 \sqrt{K_1} p_{CO_2} \sqrt{p_{H_2}} \left(1 - \frac{p_{CO} p_{H_2O}}{p_{H_2} p_{CO_2} K_{eq,RWGS}}\right)}{\left(1 + \sqrt{K_1 p_{H_2}} + K_2 K_3 p_{CO_2} \sqrt{K_1 p_{H_2}} + \frac{p_{CO}}{K_5} + \frac{p_{H_2O}}{K_{11} K_{12} \sqrt{K_1 p_{H_2}}}\right)^2} \quad (88)$$

Grouping using the adsorption constants

$$-r_{CO_2} = \frac{k_4 p_{CO_2} p_{H_2}^{0.5} \left(1 - \frac{p_{CO} p_{H_2O}}{p_{H_2} p_{CO_2} K_{eq,RWGS}}\right)}{\left(1 + \sqrt{K_{H_2} p_{H_2}} + K_{CO_2} p_{CO_2} \sqrt{K_{H_2} p_{H_2}} + K_{OH} \frac{p_{H_2O}}{p_{H_2}^{0.5}} + K_{CO} p_{CO}\right)^2} \quad (89)$$

CH_4 formation rate is derived in the same way from elementary step 6:

$$r_{CH_4} = r_6 = k_6 \Theta_{CO} \Theta_H \quad (90)$$

Substituting the carbonyl (equation (82)) and hydrogen (equation (76)) coverages expressions defined above:

$$r_{CH_4} = k_6 \frac{p_{CO}}{K_5} \Theta_* \sqrt{K_1 p_{H_2}} \Theta_* \rightarrow r_{CH_4} = k_6 \frac{\sqrt{K_1}}{K_5} p_{CO} p_{H_2}^{0.5} \Theta_*^2 \quad (91)$$

Considering the same fraction of free active sites and grouping using the adsorption constants, then:

$$r_{CH_4} = \frac{k_4 p_{CO} p_{H_2}^{0.5} \left(1 - \frac{p_{CH_4} p_{H_2O}}{p_{CO} p_{H_2}^3 K_{eq,CO-meth}}\right)}{\left(1 + \sqrt{K_{H_2} p_{H_2}} + K_{CO_2} p_{CO_2} \sqrt{K_{H_2} p_{H_2}} + K_{OH} \frac{p_{H_2O}}{p_{H_2}^{0.5}} + K_{CO} p_{CO}\right)^2} \quad (92)$$

6.3. Model M3

The following Langmuir assumptions were made for the derivation of the next kinetic model: energy uniformity of active sites, monomolecular adsorbed layer, negligible interactions between adsorbed particles, reversibility and validity of the mass action law.

Table S12. Reaction steps M3 model

Step	Reaction	Characteristics
(1)	$H_2(g) + * \leftrightarrow H_2^*$	Reversible
(2)	$H_2^* + * \leftrightarrow 2H^*$	Reversible
(3)	$CO_2(g) + * \leftrightarrow CO_2^*$	Reversible
(4)	$CO_2^* + H^* \leftrightarrow COOH^* + *$	Reversible
(5)	$COOH^* + * \leftrightarrow CO^* + OH^*$	**RDS**
(6)	$CO^* \leftrightarrow CO(g) + *$	Reversible
(7)	$CO^* + H^* \leftrightarrow C^* + OH^*$	**RDS**
(8)	$C^* + H^* \leftrightarrow CH^* + *$	Reversible
(9)	$CH^* + H^* \leftrightarrow CH_2^* + *$	Reversible
(10)	$CH_2^* + H^* \leftrightarrow CH_3^* + *$	Reversible
(11)	$CH_3^* + H^* \leftrightarrow CH_4^* + *$	Reversible
(12)	$CH_4^* \leftrightarrow CH_4(g) + *$	Reversible
(13)	$OH^* + H^* \leftrightarrow H_2O^* + *$	Reversible
(14)	$H_2O^* \leftrightarrow H_2O(g) + *$	Reversible

For all reaction steps, the kinetic expressions are derived:

(1) Hydrogen adsorption on active sites:

$$H_2 + \Theta_* \leftrightarrow \Theta_{H_2} \tag{93}$$

$$r_1 = -k_1 p_{H_2} \Theta_* + k_{-1} \Theta_{H_2} = -k_1 \left(p_{H_2} \Theta_* - \frac{k_{-1}}{k_1} \Theta_{H_2} \right) = -k_1 \left(p_{H_2} \Theta_* - \frac{\Theta_{H_2}}{K_1} \right) \tag{94}$$

(2) Hydrogen dissociation into atoms:

$$\Theta_{H_2} + \Theta_* \leftrightarrow 2\Theta_H \tag{95}$$

$$r_2 = -k_2\Theta_{H_2}\Theta_* + k_{-2}\Theta_H^2 = -k_2\left(\Theta_{H_2}\Theta_* - \frac{k_{-2}}{k_2}\Theta_H^2\right) = -k_2\left(\Theta_{H_2}\Theta_* - \frac{\Theta_H^2}{K_2}\right) \tag{96}$$

(3) Carbon dioxide adsorption on active sites:

$$CO_2 + \Theta_* \leftrightarrow \Theta_{CO_2} \tag{97}$$

$$r_3 = -k_3 p_{CO_2}\Theta_* + k_{-3}\Theta_{CO_2} = -k_3\left(p_{CO_2}\Theta_* - \frac{k_{-3}}{k_3}\Theta_{CO_2}\right) = -k_3\left(p_{CO_2}\Theta_* - \frac{\Theta_{CO_2}}{K_3}\right) \tag{98}$$

(4) Reaction with formation of the carboxyl group:

$$\Theta_{CO_2} + \Theta_H \leftrightarrow \Theta_{COOH} + \Theta_* \tag{99}$$

$$r_4 = -k_4\Theta_{CO_2}\Theta_H + k_{-4}\Theta_{\mathrm{COOH}}\Theta_* = -k_4\left(\Theta_{CO_2}\Theta_H - \frac{k_{-4}}{k_4}\Theta_{\mathrm{COOH}}\Theta_*\right) = -k_4\left(\Theta_{CO_2}\Theta_H - \frac{\Theta_{\mathrm{COOH}}\Theta_*}{K_4}\right) \tag{100}$$

(5) Carboxyl group dissociation with carbonyl group formation:

$$\Theta_{COOH} + \Theta_* \leftrightarrow \Theta_{CO} + \Theta_{OH} \tag{101}$$

$$r_5 = -k_5\Theta_{COOH}\Theta_* + k_{-5}\Theta_{\mathrm{CO}}\Theta_{OH} \tag{102}$$

(6) Carbon monoxide desorption:

$$\Theta_{CO} \leftrightarrow p_{CO} + \Theta_* \tag{103}$$

$$r_6 = -k_6\Theta_{\mathrm{CO}} + k_{-6}p_{\mathrm{CO}}\Theta_* = -k_{-6}\left(\frac{k_6}{k_{-6}}\Theta_{\mathrm{CO}} - p_{\mathrm{CO}}\Theta_*\right) = -k_{-6}\left(\frac{\Theta_{\mathrm{CO}}}{K_6} - p_{\mathrm{CO}}\Theta_*\right) \tag{104}$$

(7) Reaction with formation of solid carbon:

$$\Theta_{CO} + \Theta_H \leftrightarrow \Theta_C + \Theta_{OH} \tag{105}$$

$$r_7 = -k_7\Theta_{CO}\Theta_H + k_{-7}\Theta_{\mathrm{C}}\Theta_{OH} \tag{106}$$

(8) Hydrogenation reactions of solid carbon to the formation of carbyne:

$$\Theta_C + \Theta_H \leftrightarrow \Theta_{CH} + \Theta_* \tag{107}$$

$$r_8 = -k_8\Theta_{\mathrm{C}}\Theta_{\mathrm{H}} + k_{-8}\Theta_{\mathrm{CH}}\Theta_* = -k_8\left(\Theta_{\mathrm{C}}\Theta_{\mathrm{H}} - \frac{k_{-8}}{k_8}\Theta_{\mathrm{CH}}\Theta_*\right) = -k_8\left(\Theta_{\mathrm{C}}\Theta_{\mathrm{H}} - \frac{\Theta_{\mathrm{CH}}\Theta_*}{K_8}\right) \tag{108}$$

(9) Carbene formation reaction:

$$\Theta_{\mathrm{CH}} + \Theta_H \leftrightarrow \Theta_{CH_2} + \Theta_* \tag{109}$$

$$r_9 = -k_9\Theta_{\mathrm{CH}}\Theta_{\mathrm{H}} + k_{-9}\Theta_{CH_2}\Theta_* = -k_9\left(\Theta_{\mathrm{CH}}\Theta_{\mathrm{H}} - \frac{k_{-9}}{k_9}\Theta_{CH_2}\Theta_*\right) = -k_9\left(\Theta_{\mathrm{CH}}\Theta_{\mathrm{H}} - \frac{\Theta_{CH_2}\Theta_*}{K_9}\right) \quad (110)$$

(10) Methyl radical formation reaction:

$$\Theta_{CH_2} + \Theta_H \leftrightarrow \Theta_{CH_3} + \Theta_* \quad (111)$$

$$r_{10} = -k_{10}\Theta_{CH_2}\Theta_H + k_{-10}\Theta_{CH_3}\Theta_* = -k_{10}\left(\Theta_{CH_2}\Theta_H - \frac{k_{-10}}{k_{10}}\Theta_{CH_3}\Theta_*\right) = -k_{10}\left(\Theta_{CH_2}\Theta_H - \frac{\Theta_{CH_3}\Theta_*}{K_{10}}\right) \quad (112)$$

(11) Reaction with formation of methane:

$$\Theta_{CH_3} + \Theta_H \leftrightarrow \Theta_{CH_4} + \Theta_* \quad (113)$$

$$r_{11} = -k_{11}\Theta_{CH_3}\Theta_H + k_{-11}\Theta_{CH_4}\Theta_* = -k_{11}\left(\Theta_{CH_3}\Theta_H - \frac{k_{-11}}{k_{11}}\Theta_{CH_4}\Theta_*\right) = -k_{11}\left(\Theta_{CH_3}\Theta_H - \frac{\Theta_{CH_4}\Theta_*}{K_{11}}\right) \quad (114)$$

(12) Methane desorption:

$$\Theta_{CH_4} \leftrightarrow CH_4 + \Theta_* \quad (115)$$

$$r_{12} = -k_{12}\Theta_{CH_4} + k_{-12}p_{CH_4}\Theta_* = -k_{-12}\left(\frac{k_{12}}{k_{-12}}\Theta_{CH_4} - p_{CH_4}\Theta_*\right) = -k_{-12}\left(\frac{\Theta_{CH_4}}{K_{12}} - p_{CH_4}\Theta_*\right) \quad (116)$$

(13) Reaction with formation of water:

$$\Theta_{OH} + \Theta_H \leftrightarrow \Theta_{H_2O} + \Theta_* \quad (117)$$

$$r_{13} = -k_{13}\Theta_{\mathrm{OH}}\Theta_H + k_{-13}\Theta_{H_2O}\Theta_* = -k_{13}\left(\Theta_{\mathrm{OH}}\Theta_H - \frac{k_{-13}}{k_{13}}\Theta_{H_2O}\Theta_*\right) = -k_{13}\left(\Theta_{\mathrm{OH}}\Theta_H - \frac{\Theta_{H_2O}\Theta_*}{K_{13}}\right) \quad (118)$$

(14) Water desorption:

$$\Theta_{H_2O} \leftrightarrow H_2\mathrm{O} + \Theta_* \quad (119)$$

$$r_{14} = -k_{14}\Theta_{H_2O} + k_{-14}p_{H_2O}\Theta_* = -k_{-14}\left(\frac{k_{14}}{k_{-14}}\Theta_{H_2O} - p_{H_2O}\Theta_*\right) = -k_{-14}\left(\frac{\Theta_{H_2O}}{K_{14}} - p_{H_2O}\Theta_*\right) \quad (120)$$

The dissociation of the carboxyl group (equation (102)) and the formation of solid carbon from carbon monoxide (equation (106)) are considered RDS. For all other intermediate reactions, the assumption of Langmuir stationarity is applied. The following species are assumed as MASI:

$$1 = \Theta_* + \Theta_H + \Theta_{\mathrm{CO}} + \Theta_C + \Theta_{CH_4} \quad (121)$$

Coverage fractions can be derived from the individual reaction steps.

The hydrogen coverage fraction can be derived from equation (96):

$$\Theta_{H_2} = K_1 p_{H_2} \Theta_* \tag{122}$$

$$\Theta_H = \left(K_2 \Theta_{H_2} \Theta_*\right)^{0.5} = \left(K_2 K_1 p_{H_2}\right)^{0.5} \Theta_* = K_{H_2}^{0.5} p_{H_2}^{0.5} \Theta_* \tag{123}$$

The coverage fraction of carbon monoxide can be derived from equation (104):

$$\Theta_{CO} = K_{\mathrm{CO}} p_{\mathrm{CO}} \Theta_* \tag{124}$$

The coverage fraction of solid carbon can be derived from equation (108):

$$\Theta_{\mathrm{C}} = \frac{\Theta_{\mathrm{CH}} \Theta_*}{K_8 \Theta_{\mathrm{H}}} \tag{125}$$

$$\Theta_{\mathrm{C}} = K_{\mathrm{C}} \frac{p_{CH_4} \Theta_*}{p_{H_2}^2} \tag{126}$$

The coverage fraction of methane is derived by considering Langmuir desorption reaction of methane (Equation (116)):

$$\Theta_{CH_4} = K_{CH_4} p_{CH_4} \Theta_* \tag{127}$$

Substituting the expressions found in equation (121):

$$1 = \Theta_* + K_{H_2}^{0.5} p_{H_2}^{0.5} \Theta_* + K_{\mathrm{CO}} p_{\mathrm{CO}} \Theta_* + K_{\mathrm{C}} \frac{p_{CH_4} \Theta_*}{p_{H_2}^2} + K_{CH_4} p_{CH_4} \Theta_\sigma \tag{128}$$

$$\Theta_* = \frac{1}{1 + K_{H_2}^{0.5} p_{H_2}^{0.5} + K_{\mathrm{CO}} p_{\mathrm{CO}} + K_{\mathrm{C}} \frac{p_{CH_4}}{p_{H_2}^2} + K_{CH_4} p_{CH_4}} \tag{129}$$

The formation of CO from CO_2 is derived from:

$$r_5 = -k_5 \Theta_{COOH} \Theta_* + k_{-5} \Theta_{\mathrm{CO}} \Theta_{OH} \tag{130}$$

Θ_{COOH} is derived from Equation (100):

$$\Theta_{\mathrm{COOH}} = K_{\mathrm{COOH}} p_{CO_2} p_{H_2}^{0.5} \Theta_* \tag{131}$$

Θ_{OH} is derived from Equation (118):

$$\Theta_{OH} = K_{\mathrm{OH}} \frac{p_{H_2O}}{p_{H_2}^{0.5}} \Theta_* \tag{132}$$

Substituting these expressions into the kinetic expression (102):

$$r_5 = -k_5 K_{\mathrm{COOH}} p_{CO_2} p_{H_2}^{0.5} \Theta_*^2 + -k_{-5} K_{\mathrm{CO}} p_{\mathrm{CO}} K_{\mathrm{OH}} \frac{p_{H_2O}}{p_{H_2}^{0.5}} \Theta_*^2 \tag{133}$$

$$r_5 = -k_5 K_{\mathrm{COOH}} p_{CO_2} p_{H_2}^{0.5} \Theta_*^2 \left(1 - \frac{k_{-5} K_{\mathrm{CO}} K_{\mathrm{OH}}}{k_5 K_{\mathrm{COOH}}} \frac{p_{\mathrm{CO}} p_{H_2O}}{p_{CO_2} p_{H_2}}\right) \tag{134}$$

Grouping the constants together gives:

$$r_{\mathrm{RWGS}} = \frac{k_{\mathrm{RWGS}} p_{CO_2} p_{H_2}^{0.5}}{\left(1 + K_{H_2}^{0.5} p_{H_2}^{0.5} + K_{\mathrm{CO}} p_{\mathrm{CO}} + K_{\mathrm{C}} \frac{p_{CH_4}}{p_{H_2}^2} + K_{CH_4} p_{CH_4}\right)^2} \left(1 - \frac{Q_{\mathrm{RWGS}}}{K_{eq,\mathrm{RWGS}}}\right) \tag{135}$$

Methane formation rate:

$$r_7 = -k_7 \Theta_{CO} \Theta_H + k_{-7} \Theta_{\mathrm{C}} \Theta_{OH} \tag{136}$$

By substituting adsorption fractions:

$$r_7 = -k_7 K_{\mathrm{CO}} p_{\mathrm{CO}} K_{H_2}^{0.5} p_{H_2}^{0.5} \Theta_*^2 + k_{-7} K_{\mathrm{C}} \frac{p_{CH_4}}{p_{H_2}^2} K_{\mathrm{OH}} \frac{p_{H_2O}}{p_{H_2}^{0.5}} \Theta_*^2 \tag{137}$$

$$r_7 = -k_7 K_{\mathrm{CO}} p_{\mathrm{CO}} K_{H_2}^{0.5} p_{H_2}^{0.5} \Theta_*^2 \left(1 - \frac{k_{-7} K_{\mathrm{C}} K_{\mathrm{OH}}}{k_7 K_{\mathrm{CO}} K_{H_2}^{0.5}} \frac{p_{CH_4} p_{H_2O}}{p_{\mathrm{CO}} p_{H_2}^3}\right) \tag{138}$$

Grouping the constants together gives:

$$r_{\mathrm{CO-meth}} = \frac{k_{\mathrm{CO-meth}} p_{\mathrm{CO}} p_{H_2}^{0.5}}{\left(1 + K_{H_2}^{0.5} p_{H_2}^{0.5} + K_{\mathrm{CO}} p_{\mathrm{CO}} + K_{\mathrm{C}} \frac{p_{CH_4}}{p_{H_2}^2} + K_{CH_4} p_{CH_4}\right)^2} \left(1 - \frac{Q_{\mathrm{CO-meth}}}{K_{eq,\mathrm{CO-meth}}}\right) \tag{139}$$

Grouping together the kinetics found, methane formation is described by Equation (139), and carbon monoxide formation by Equation (135).

6.4. Model M4

The steps proposed in M1 (Koschany) and M3 were considered for the derivation of this model.

Table S13. Reaction steps M4 model

Step	Reactions	Characteristics
(1)	$H_2(\mathrm{g}) + * \leftrightarrow H_2^*$	Reversible
(2)	$H_2^* + * \leftrightarrow 2H^*$	Reversible
(3)	$CO_2(\mathrm{g}) + * \leftrightarrow CO_2^*$	Reversible
(4)	$CO_2^* + H^* \leftrightarrow COOH^* + *$	Reversible
(5)	$COOH^* + * \leftrightarrow CO^* + OH^*$	**RDS**
(6)	$CO_2(\mathrm{g}) + 2* \leftrightarrow CO^* + O^*$	Reversible
(7)	$CO^* \leftrightarrow \mathrm{CO(g)} + *$	Reversible
(8)	$CO^* + H^* \leftrightarrow C^* + OH^*$	**RDS**
(9)	$C^* + H^* \leftrightarrow CH^* + *$	Reversible
(10)	$CO^* + H^* \leftrightarrow CHO^* + *$	**RDS**
(11)	$CHO^* + * \leftrightarrow CH^* + O^*$	Reversible
(12)	$CH^* + H^* \leftrightarrow CH_2^* + *$	Reversible
(13)	$CH_2^* + H^* \leftrightarrow CH_3^* + *$	Reversible
(14)	$CH_3^* + H^* \leftrightarrow CH_4^* + *$	Reversible
(15)	$CH_4^* \leftrightarrow CH_4(g) + *$	Reversible
(16)	$O^* + H^* \leftrightarrow OH^* + *$	Reversible
(17)	$OH^* + H^* \leftrightarrow H_2O^* + *$	Reversible
(18)	$H_2O^* \leftrightarrow H_2O(g) + *$	Reversible

The same MASI are considered and therefore the same expression is obtained as in the Equation (121).

The RWGS reaction and the rate of methane formation from carbon monoxide are derived using the same methodology as the M3 model, assuming the same RDS. The kinetic expressions obtained are the same as those given in Equation (135) and Equation (139), respectively:

$$r_{\mathrm{RWGS}} = \frac{k_{\mathrm{RWGS}} p_{CO_2} p_{H_2}^{0.5}}{\left(1 + K_{H_2}^{0.5} p_{H_2}^{0.5} + K_{\mathrm{CO}} p_{\mathrm{CO}} + K_{\mathrm{C}} \frac{p_{CH_4}}{p_{H_2}^2} + K_{CH_4} p_{CH_4}\right)^2} \left(1 - \frac{Q_{\mathrm{RWGS}}}{K_{eq,\mathrm{RWGS}}}\right) \quad (140)$$

$$r_{\mathrm{CO-meth}} = \frac{k_{\mathrm{CO-meth}} p_{\mathrm{CO}} p_{H_2}^{0.5}}{\left(1 + K_{H_2}^{0.5} p_{H_2}^{0.5} + K_{\mathrm{CO}} p_{\mathrm{CO}} + K_{\mathrm{C}} \frac{p_{CH_4}}{p_{H_2}^2} + K_{CH_4} p_{CH_4}\right)^2} \left(1 - \frac{Q_{\mathrm{CO-meth}}}{K_{eq,\mathrm{CO-meth}}}\right) \quad (141)$$

Rate of methane formation from carbon dioxide:

$$r_{10} = -k_{10} \Theta_{\mathrm{CO}} \Theta_{\mathrm{H}} + k_{-10} \Theta_{\mathrm{CHO}} \Theta_* \quad (142)$$

In this case the carbon monoxide coverage fraction is derived from the dissociation of CO_2, step (6):

$$\Theta_{CO} = K_{\mathrm{CO}} \frac{p_{CO_2}}{\Theta_{\mathrm{O}}} \Theta_*^2 \quad (143)$$

Θ_{O} is derived from step (16):

$$\Theta_O = \frac{\Theta_{\mathrm{OH}} \Theta_*}{K_{16} \Theta_{\mathrm{H}}} \quad (144)$$

The expression of Θ_{OH} is reported in Equation (132). Substituting the expression into Equation (144):

$$\Theta_O = K_O \frac{p_{H_2O}}{p_{H_2}} \Theta_* \quad (145)$$

By substituting the expression (145), into Equation (143):

$$\Theta_{CO} = K_{\mathrm{CO}} \frac{p_{CO_2} p_{H_2}}{p_{H_2O}} \Theta_* \quad (146)$$

Θ_{CHO} is derived from step (11):

$$\Theta_{CHO} = \frac{\Theta_{CH} \Theta_O}{K_{11} \Theta_*} \quad (147)$$

Θ_{CH} is derived from step (12), as reported in Equation (110):

$$\Theta_{CH} = K_{CH} \frac{p_{CH_4} \Theta_*}{p_{H_2}^{1.5}} \quad (148)$$

By substituting the expression (148), into Equation (147):

$$\Theta_{CHO} = K_{CHO} \frac{p_{CH_4} p_{H_2O}}{p_{H_2}^{2.5}} \Theta_* \quad (149)$$

At this point, substituting the equations (123), (143) and (149) into equation (142) the kinetic expression becomes:

$$r_{10} = -k_{10}K_{\mathrm{CO}}\frac{p_{CO_2}p_{H_2}}{p_{H_2O}}\Theta_* K_{H_2}^{0.5}p_{H_2}^{0.5}\Theta_* + k_{-10}K_{CHO}\frac{p_{CH_4}p_{H_2O}}{p_{H_2}^{2.5}}\Theta_*\Theta_* \tag{150}$$

$$r_{10} = -k_{10}K_{\mathrm{CO}}K_{H_2}^{0.5}\frac{p_{CO_2}p_{H_2}^{1.5}}{p_{H_2O}}\Theta_*^2 + k_{-10}K_{CHO}\frac{p_{CH_4}p_{H_2O}}{p_{H_2}^{2.5}}\Theta_*^2 \tag{151}$$

$$r_{10} = -k_{10}K_{\mathrm{CO}}K_{H_2}^{0.5}\frac{p_{CO_2}p_{H_2}^{1.5}}{p_{H_2O}}\Theta_*^2\left(1 - \frac{k_{-10}K_{CHO}}{k_{10}K_{\mathrm{CO}}K_{H_2}^{0.5}}\frac{p_{CH_4}p_{H_2O}^2}{p_{CO_2}p_{H_2}^4}\right) \tag{152}$$

Grouping all the constants:

$$r_{\mathrm{CO2-meth}} = \frac{k_{\mathrm{CO2-meth}}\dfrac{p_{CO_2}p_{H_2}^{1.5}}{p_{H_2O}}}{\left(1 + K_{H_2}^{0.5}p_{H_2}^{0.5} + K_{\mathrm{CO}}p_{\mathrm{CO}} + K_{\mathrm{C}}\dfrac{p_{CH_4}}{p_{H_2}^2} + K_{CH_4}p_{CH_4}\right)^2}\left(1 - \frac{Q_{\mathrm{CO2-meth}}}{K_{eq,\mathrm{CO2-meth}}}\right) \tag{153}$$

Summarizing the results, methane and carbon monoxide production rate are described by the following expressions:

$$r_{\mathrm{CO2-meth}} = \frac{k_{\mathrm{CO2-meth}}\dfrac{p_{CO_2}p_{H_2}^{1.5}}{p_{H_2O}}}{\left(1 + K_{H_2}^{0.5}p_{H_2}^{0.5} + K_{\mathrm{CO}}p_{\mathrm{CO}} + K_{\mathrm{C}}\dfrac{p_{CH_4}}{p_{H_2}^2} + K_{CH_4}p_{CH_4}\right)^2}\left(1 - \frac{Q_{\mathrm{CO2-meth}}}{K_{eq,\mathrm{CO2-meth}}}\right) \tag{154}$$

$$r_{\mathrm{RWGS}} = \frac{k_{\mathrm{RWGS}}p_{CO_2}p_{H_2}^{0.5}}{\left(1 + K_{H_2}^{0.5}p_{H_2}^{0.5} + K_{\mathrm{CO}}p_{\mathrm{CO}} + K_{\mathrm{C}}\dfrac{p_{CH_4}}{p_{H_2}^2} + K_{CH_4}p_{CH_4}\right)^2}\left(1 - \frac{Q_{\mathrm{RWGS}}}{K_{eq,\mathrm{RWGS}}}\right) \tag{155}$$

$$r_{\mathrm{CO-meth}} = \frac{k_{\mathrm{CO-meth}}p_{\mathrm{CO}}p_{H_2}^{0.5}}{\left(1 + K_{H_2}^{0.5}p_{H_2}^{0.5} + K_{\mathrm{CO}}p_{\mathrm{CO}} + K_{\mathrm{C}}\dfrac{p_{CH_4}}{p_{H_2}^2} + K_{CH_4}p_{CH_4}\right)^2}\left(1 - \frac{Q_{\mathrm{CO-meth}}}{K_{eq,\mathrm{CO-meth}}}\right) \tag{156}$$

6.5. Model M5

Table S14. Reaction steps M5 model

Step	Reactions	Characteristics
(1)	$H_2(\mathrm{g}) + * \leftrightarrow H_2^*$	Reversible
(2)	$H_2^* + * \leftrightarrow 2H^*$	Reversible
(3)	$CO_2(\mathrm{g}) + * \leftrightarrow CO_2^*$	Reversible
(4)	$CO(g) + * \leftrightarrow CO^*$	Reversible
(5)	$CO_2^* + H^* \leftrightarrow CHO^* + O^*$	**RDS**
(6)	$CO_2^* + * \leftrightarrow CO^* + O^*$	**RDS**
(7)	$CO^* + H^* \leftrightarrow CHO^* + *$	**RDS**
(8)	$CHO^* + H^* \leftrightarrow CH_2O^* + *$	Reversible
(9)	$CH_2O^* + * \leftrightarrow CH_2{}^* + O^*$	Reversible
(10)	$CH_2{}^* + H^* \leftrightarrow CH_3{}^* + *$	Reversible
(11)	$CH_3{}^* + H^* \leftrightarrow CH_4{}^* + *$	Reversible
(12)	$CH_4{}^* \leftrightarrow CH_4(g) + *$	Reversible
(13)	$H_2(g) + O^* \leftrightarrow H_2O(g) + *$	Reversible

For all reaction steps, the kinetic expressions are derived:

(1) Hydrogen adsorption on active sites:

$$H_2 + \Theta_* \leftrightarrow 2\Theta_{H_2} \tag{157}$$

$$r_1 = -k_1 p_{H_2} \Theta_* + k_{-1} \Theta_{H_2} = -k_1 \left(p_{H_2} \Theta_* - \frac{k_{-1}}{k_1} \Theta_{H_2} \right) = -k_1 \left(p_{H_2} \Theta_* - \frac{\Theta_{H_2}}{K_1} \right) \tag{158}$$

(2) Hydrogen dissociation into atoms:

$$\Theta_{H_2} + \Theta_\sigma \leftrightarrow 2\Theta_H \tag{159}$$

$$r_2 = -k_2 \Theta_{H_2} \Theta_\sigma + k_{-2} \Theta_H^2 = -k_2 \left(\Theta_{H_2} \Theta_\sigma - \frac{k_{-2}}{k_2} \Theta_H^2 \right) = -k_2 \left(\Theta_{H_2} \Theta_\sigma - \frac{\Theta_H^2}{K_2} \right) \tag{160}$$

(3) Carbon dioxide adsorption on active sites:

$$CO_2 + \Theta_* \leftrightarrow \Theta_{CO_2} \tag{161}$$

$$r_3 = -k_3 p_{CO_2} \Theta_* + k_{-3} \Theta_{CO_2} = -k_3 \left(p_{CO_2} \Theta_* - \frac{k_{-3}}{k_3} \Theta_{CO_2} \right) = -k_3 \left(p_{CO_2} \Theta_* - \frac{\Theta_{CO_2}}{K_3} \right) \tag{162}$$

(4) Carbon monoxide adsorption on active sites:

$$CO + \Theta_* \leftrightarrow \Theta_{CO} \tag{163}$$

$$r_4 = -k_4 p_{CO} \Theta_* + k_{-4} \Theta_{CO} = -k_4 \left(p_{CO} \Theta_* - \frac{k_{-4}}{k_4} \Theta_{CO} \right) = -k_4 \left(p_{CO} \Theta_* - \frac{\Theta_{CO}}{K_4} \right) \tag{164}$$

(5) Hydrogenation of carbon dioxide with formation of the formyl group:

$$\Theta_{CO_2} + \Theta_H \leftrightarrow \Theta_{CHO} + \Theta_O \tag{165}$$

$$r_5 = -k_5 \Theta_{CO_2} \Theta_H + k_{-5} \Theta_{CHO} \Theta_O \tag{166}$$

(6) Carbon dioxide dissociation reaction:

$$\Theta_{CO_2} + \Theta_\sigma \leftrightarrow \Theta_{CO} + \Theta_O \tag{167}$$

$$r_6 = -k_6 \Theta_{CO_2} \Theta_\sigma + k_{-6} \Theta_{CO} \Theta_O \tag{168}$$

(7) Hydrogenation of carbon monoxide with formation of the formyl group:

$$\Theta_{CO} + \Theta_H \leftrightarrow \Theta_{CHO} + \Theta_* \tag{169}$$

$$r_7 = -k_7 \Theta_{CO} \Theta_H + k_{-7} \Theta_{CHO} \Theta_* \tag{170}$$

(8) Hydroxycarbene reaction formation:

$$\Theta_{CHO} + \Theta_H \leftrightarrow \Theta_{CH_2O} + \Theta_* \tag{171}$$

$$r_8 = -k_8 \Theta_{CHO} \Theta_H + k_{-8} \Theta_{CH_2O} \Theta_* = -k_8 \left(\Theta_{CHO} \Theta_H - \frac{k_{-8}}{k_8} \Theta_{CH_2O} \Theta_* \right) = -k_8 \left(\Theta_{CHO} \Theta_H - \frac{\Theta_{CH_2O} \Theta_*}{K_8} \right) \tag{172}$$

(9) Carbene formation reaction:

$$\Theta_{CH_2O} + \Theta_* \leftrightarrow \Theta_{CH_2} + \Theta_O \tag{173}$$

$$r_9 = -k_9 \Theta_{CH_2O} \Theta_* + k_{-9} \Theta_{CH_2} \Theta_O = -k_9 \left(\Theta_{CH_2O} \Theta_* - \frac{k_{-9}}{k_9} \Theta_{CH_2} \Theta_O \right) = -k_9 \left(\Theta_{CH_2O} \Theta_* - \frac{\Theta_{CH_2} \Theta_O}{K_9} \right) \tag{174}$$

(10) methyl radical formation reaction:

$$\Theta_{CH_2} + \Theta_H \leftrightarrow \Theta_{CH_3} + \Theta_* \tag{175}$$

$$r_{10} = -k_{10} \Theta_{CH_2} \Theta_H + k_{-10} \Theta_{CH_3} \Theta_* = -k_{10} \left(\Theta_{CH_2} \Theta_H - \frac{k_{-10}}{k_{10}} \Theta_{CH_3} \Theta_* \right) = -k_{10} \left(\Theta_{CH_2} \Theta_H - \frac{\Theta_{CH_3} \Theta_*}{K_{10}} \right) \tag{176}$$

(11) Methane formation reaction:

$$\Theta_{CH_3} + \Theta_H \leftrightarrow \Theta_{CH_4} + \Theta_* \tag{177}$$

$$r_{11} = -k_{11}\Theta_{CH_3}\Theta_H + k_{-11}\Theta_{CH_4}\Theta_* = -k_{11}\left(\Theta_{CH_3}\Theta_H - \frac{k_{-11}}{k_{11}}\Theta_{CH_4}\Theta_*\right) = -k_{11}\left(\Theta_{CH_3}\Theta_H - \frac{\Theta_{CH_4}\Theta_*}{K_{11}}\right) \tag{178}$$

(12) Methane desorption:

$$\Theta_{CH_4} \leftrightarrow CH_4 + \Theta_* \tag{179}$$

$$r_{12} = -k_{12}\Theta_{CH_4} + k_{-12}p_{CH_4}\Theta_* = -k_{-12}\left(\frac{k_{12}}{k_{-12}}\Theta_{CH_4} - p_{CH_4}\Theta_*\right) = -k_{-12}\left(\frac{\Theta_{CH_4}}{K_{12}} - p_{CH_4}\Theta_*\right) \tag{180}$$

(13) Water formation reaction:

$$H_2 + \Theta_O \leftrightarrow H_2O + \Theta_* \tag{181}$$

$$r_{13} = -k_{13}p_{H_2}\Theta_O + k_{-13}p_{H_2O}\Theta_* = -k_{-13}\left(\frac{k_{13}}{k_{-13}}p_{H_2}\Theta_O - p_{H_2O}\Theta_*\right) = -k_{-13}\left(\frac{p_{H_2}\Theta_O}{K_{13}} - p_{H_2O}\Theta_*\right) \tag{182}$$

Formation of the formyl group from both CO_2 and CO and dissociation of CO_2 are assumed as RDS. For all other intermediate reactions, the assumption of Langmuir stationarity is applied.

The following species are assumed as MASI:

$$1 = \Theta_* + \Theta_H + \Theta_{\mathrm{CO}} + \Theta_O + \Theta_{CH_4} \tag{183}$$

Coverage fractions can be derived from the individual reaction steps.

The hydrogen coverage fraction can be derived from equation (160):

$$\Theta_{H_2} = K_1 p_{H_2}\Theta_* \tag{184}$$

$$\Theta_H = \left(K_2\Theta_{H_2}\Theta_*\right)^{0.5} = \left(K_2K_1p_{H_2}\right)^{0.5}\Theta_* = K_{H_2}^{0.5}p_{H_2}^{0.5}\Theta_* \tag{185}$$

The coverage fraction of CO is derived by considering Langmuir adsorption reaction (equation (164)):

$$\Theta_{CO} = K_{\mathrm{CO}}p_{\mathrm{CO}}\Theta_* \tag{186}$$

The coverage fraction of oxygen can be derived from equation (182):

$$\Theta_{\mathrm{O}} = K_{H_2O}\frac{p_{H_2O}}{p_{H_2}}\Theta_* \tag{187}$$

The coverage fraction of methane is derived by considering Langmuir desorption reaction of methane (Equation (180)):

$$\Theta_{CH_4} = K_{CH_4} p_{CH_4} \Theta_*$$ (188)

Substituting the expressions found in equation (183):

$$1 = \Theta_* + K_{H_2}^{0.5} p_{H_2}^{0.5} \Theta_* + K_{\mathrm{CO}} p_{\mathrm{CO}} \Theta_* + K_{H_2O} \frac{p_{H_2O}}{p_{H_2}} \Theta_* + K_{CH_4} p_{CH_4} \Theta_*$$ (189)

$$\Theta_* = \frac{1}{1 + K_{H_2}^{0.5} p_{H_2}^{0.5} + K_{\mathrm{CO}} p_{\mathrm{CO}} + K_{H_2O} \frac{p_{H_2O}}{p_{H_2}} + K_{CH_4} p_{CH_4}}$$ (190)

The formation reaction of the formyl group from CO_2 is:

$$r_5 = -k_5 \Theta_{CO_2} \Theta_H + k_{-5} \Theta_{CHO} \Theta_O$$ (191)

Θ_{CHO} is derived from Equation (172):

$$\Theta_{\mathrm{CHO}} = K_{CHO} \frac{p_{CH_4} p_{H_2O}}{p_{H_2}^{2.5}} \Theta_*$$ (192)

By substituting the coverage fractions into the equation (166):

$$r_5 = -k_5 K_{CO_2} p_{CO_2} \Theta_* K_{H_2}^{0.5} p_{H_2}^{0.5} \Theta_* + k_{-5} K_{CHO} \frac{p_{CH_4} p_{H_2O}}{p_{H_2}^{2.5}} \Theta_* K_{H_2O} \frac{p_{H_2O}}{p_{H_2}} \Theta_*$$ (193)

$$r_5 = -k_5 K_{CO_2} p_{CO_2} K_{H_2}^{0.5} p_{H_2}^{0.5} \Theta_*^2 \left(1 - \frac{k_{-5} K_{CHO} K_{H_2O}}{k_5 K_{CO_2} K_{H_2}^{0.5}} \frac{p_{CH_4} p_{H_2O}}{p_{H_2}^4 p_{CO_2}}\right)$$ (194)

Grouping the constants together gives:

$$r_{\mathrm{CO2-meth}} = \frac{k_{CO2-meth} p_{CO_2} p_{H_2}^{0.5}}{\left(1 + K_{H_2}^{0.5} p_{H_2}^{0.5} + K_{CO} p_{CO} + K_{H_2O} \frac{p_{H_2O}}{p_{H_2}} + K_{CH_4} p_{CH_4}\right)^2} \left(1 - \frac{Q_{\mathrm{CO2-meth}}}{K_{eq,\mathrm{CO2-meth}}}\right)$$ (195)

The dissociation reaction of CO_2 is:

$$r_6 = -k_6 \Theta_{CO_2} \Theta_* + k_{-6} \Theta_{CO} \Theta_O$$ (196)

Θ_{CO_2} is derived from Equation (162):

$$\Theta_{CO_2} = K_{CO_2} p_{CO_2} \Theta_*$$ (197)

By substituting the coverage fractions into the equation (168):

$$r_6 = -k_6 K_{CO_2} p_{CO_2} \Theta_* \Theta_* + k_{-6} K_{CO} p_{CO} \Theta_* K_{H_2O} \frac{p_{H_2O}}{p_{H_2}} \Theta_*$$ (198)

$$r_6 = -k_6 K_{CO_2} p_{CO_2} \Theta_*^2 \left(1 - \frac{k_{-6} K_{\mathrm{CO}} K_{H_2O}}{k_6 K_{CO_2}} \frac{p_{CO} p_{H_2O}}{p_{H_2} p_{CO_2}}\right) \tag{199}$$

Grouping the constants together gives:

$$r_{\mathrm{RWGS}} = \frac{k_{RWGS} p_{CO_2}}{\left(1 + K_{H_2}^{0.5} p_{H_2}^{0.5} + K_{CO} p_{CO} + K_{H_2O} \frac{p_{H_2O}}{p_{H_2}} + K_{CH_4} p_{CH_4}\right)^2} \left(1 - \frac{Q_{RWGS}}{K_{eq,\mathrm{RWGS}}}\right) \tag{200}$$

The formation reaction of the formyl group from CO is:

$$r_7 = -k_7 \Theta_{CO} \Theta_H + k_{-7} \Theta_{CHO} \Theta_* \tag{201}$$

By substituting the coverage fractions into the equation (170):

$$r_7 = -k_7 K_{\mathrm{CO}} p_{CO} \Theta_* K_{H_2}^{0.5} p_{H_2}^{0.5} \Theta_* + k_{-7} K_{CHO} \frac{p_{CH_4} p_{H_2O}}{p_{H_2}^{2.5}} \Theta_* \Theta_* \tag{202}$$

$$r_7 = -k_7 K_{CO} K_{H_2}^{0.5} p_{H_2}^{0.5} p_{CO} \Theta_*^2 \left(1 - \frac{k_{-7} K_{CHO}}{k_7 K_{\mathrm{CO}} K_{H_2}^{0.5}} \frac{p_{CH_4} p_{H_2O}}{p_{CO} p_{H_2}^3}\right) \tag{203}$$

Grouping the constants together gives:

$$r_{\mathrm{CO-meth}} = \frac{k_{CO-meth} p_{H_2}^{0.5} p_{CO}}{\left(1 + K_{H_2}^{0.5} p_{H_2}^{0.5} + K_{CO} p_{CO} + K_{H_2O} \frac{p_{H_2O}}{p_{H_2}} + K_{CH_4} p_{CH_4}\right)^2} \left(1 - \frac{Q_{CO-meth}}{K_{eq,\mathrm{CO-meth}}}\right) \tag{204}$$

Summarizing, the formation rate of methane from carbon dioxide and carbon monoxide and the formation rate of carbon monoxide are:

$$r_{\mathrm{CO2-meth}} = \frac{k_{CO2-meth} p_{CO_2} p_{H_2}^{0.5}}{\left(1 + K_{H_2}^{0.5} p_{H_2}^{0.5} + K_{CO} p_{CO} + K_{H_2O} \frac{p_{H_2O}}{p_{H_2}} + K_{CH_4} p_{CH_4}\right)^2} \left(1 - \frac{Q_{\mathrm{CO2-meth}}}{K_{eq,\mathrm{CO2-meth}}}\right) \tag{205}$$

$$r_{\mathrm{RWGS}} = \frac{k_{RWGS} p_{CO_2}}{\left(1 + K_{H_2}^{0.5} p_{H_2}^{0.5} + K_{CO} p_{CO} + K_{H_2O} \frac{p_{H_2O}}{p_{H_2}} + K_{CH_4} p_{CH_4}\right)^2} \left(1 - \frac{Q_{RWGS}}{K_{eq,\mathrm{RWGS}}}\right) \tag{206}$$

$$r_{\mathrm{CO-meth}} = \frac{k_{CO-meth} p_{H_2}^{0.5} p_{CO}}{\left(1 + K_{H_2}^{0.5} p_{H_2}^{0.5} + K_{CO} p_{CO} + K_{H_2O} \frac{p_{H_2O}}{p_{H_2}} + K_{CH_4} p_{CH_4}\right)^2} \left(1 - \frac{Q_{CO-meth}}{K_{eq,\mathrm{CO-meth}}}\right) \tag{207}$$

7. Characterization of the catalysts

7.1. N_2 physisorption measurements

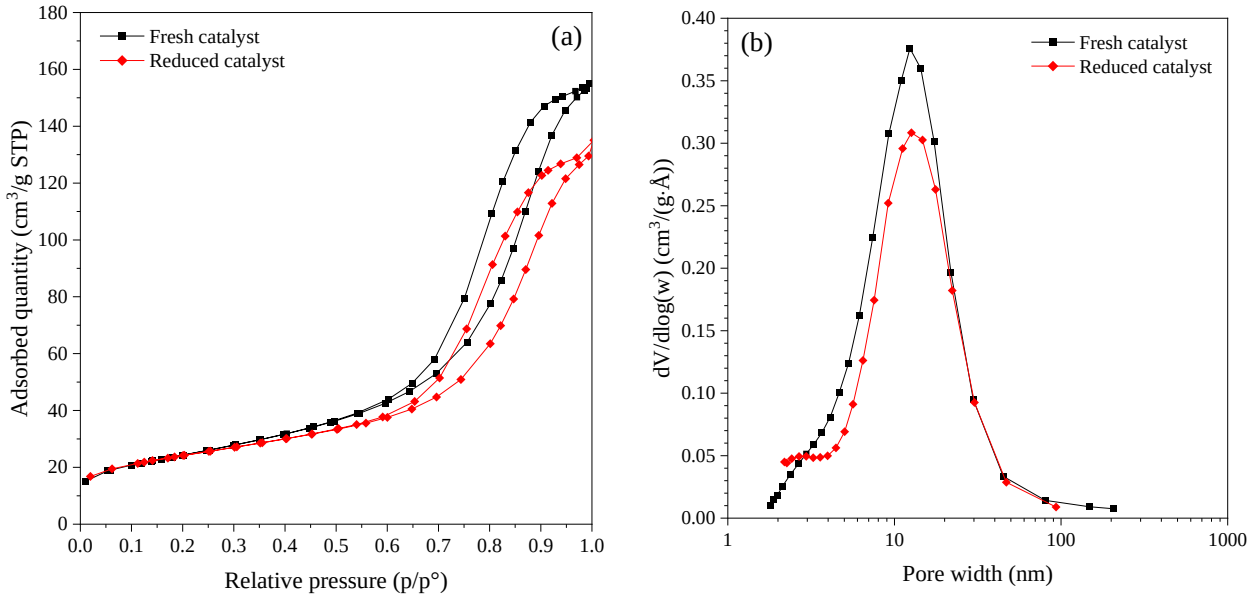

Figure S2. (a) N_2 physisorption isotherms and (b) pore size distribution of the fresh and reduced catalyst.

7.2. H_2-TPR measurements

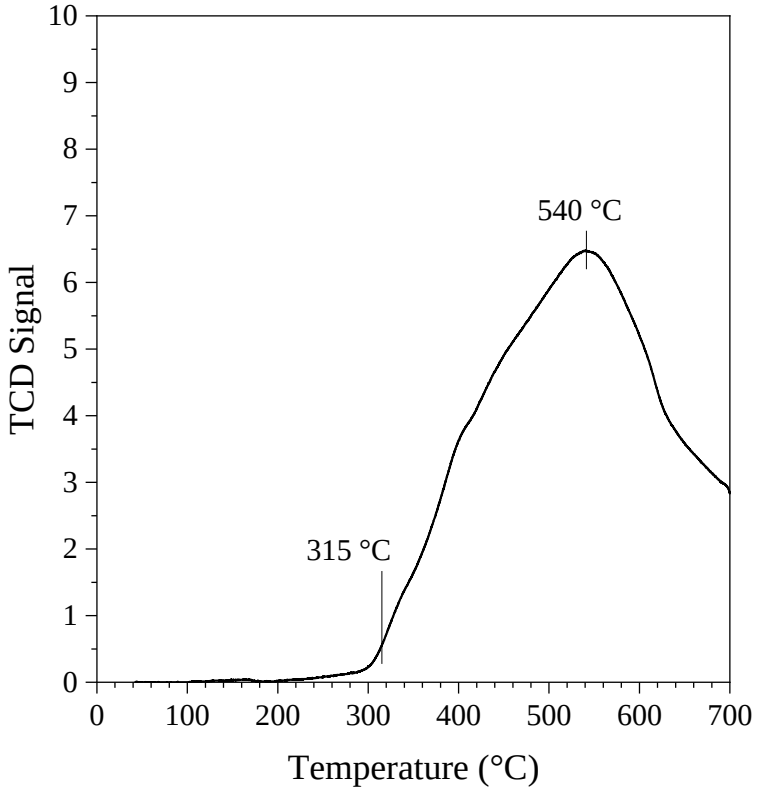

Figure S3. H_2-TPR measurement on the fresh 24 wt.% Ni/Al_2O_3 catalyst.

7.3. SEM measurements

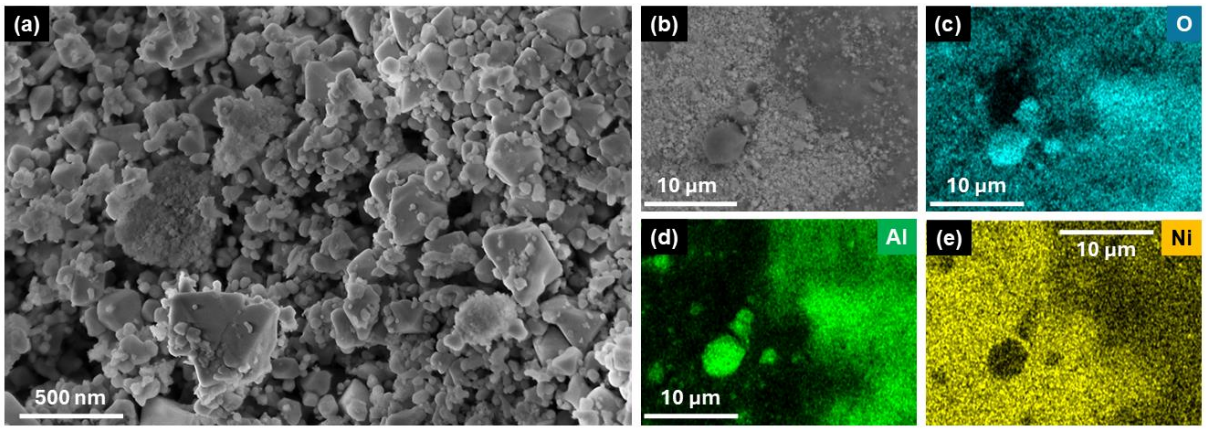

Figure S4. SEM-EDS images of the fresh NiO/Al_2O_3 catalyst at different magnifications: (a) 100 kX in SE mode, (b-e) 5 kX EDS map.

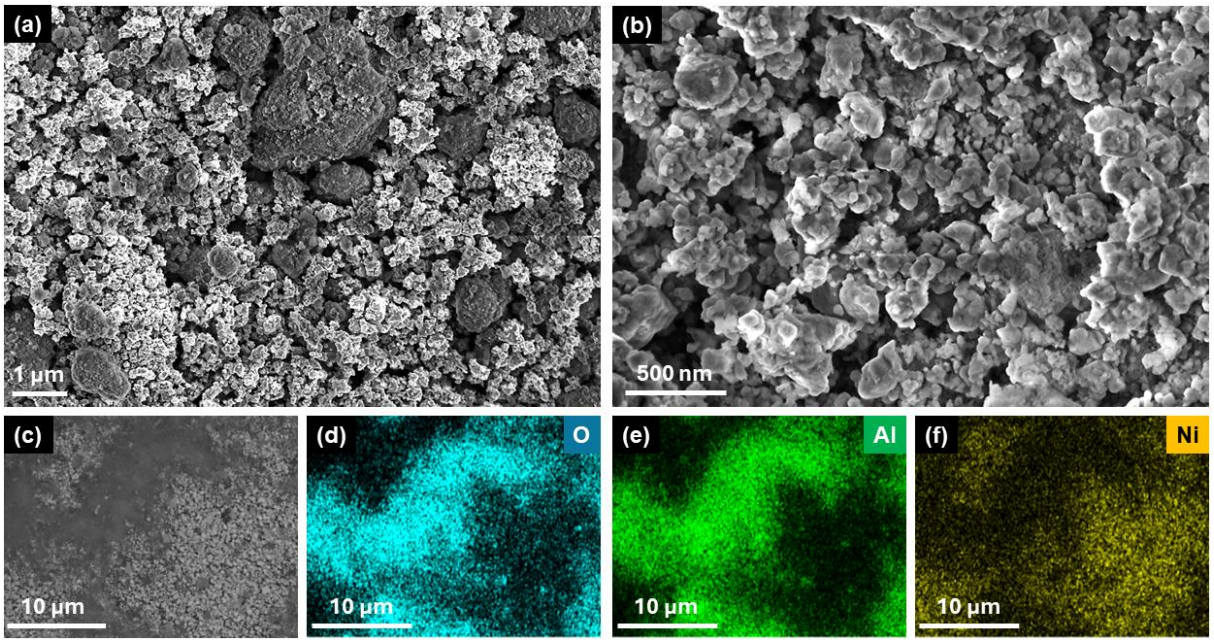

Figure S5. SEM-EDS images of the reduced catalyst at different magnifications: (a) 25 kX in SE mode, (b) 100 kX in SE mode, (c-f) 5 kX EDS map.

7.4. XRD measurements

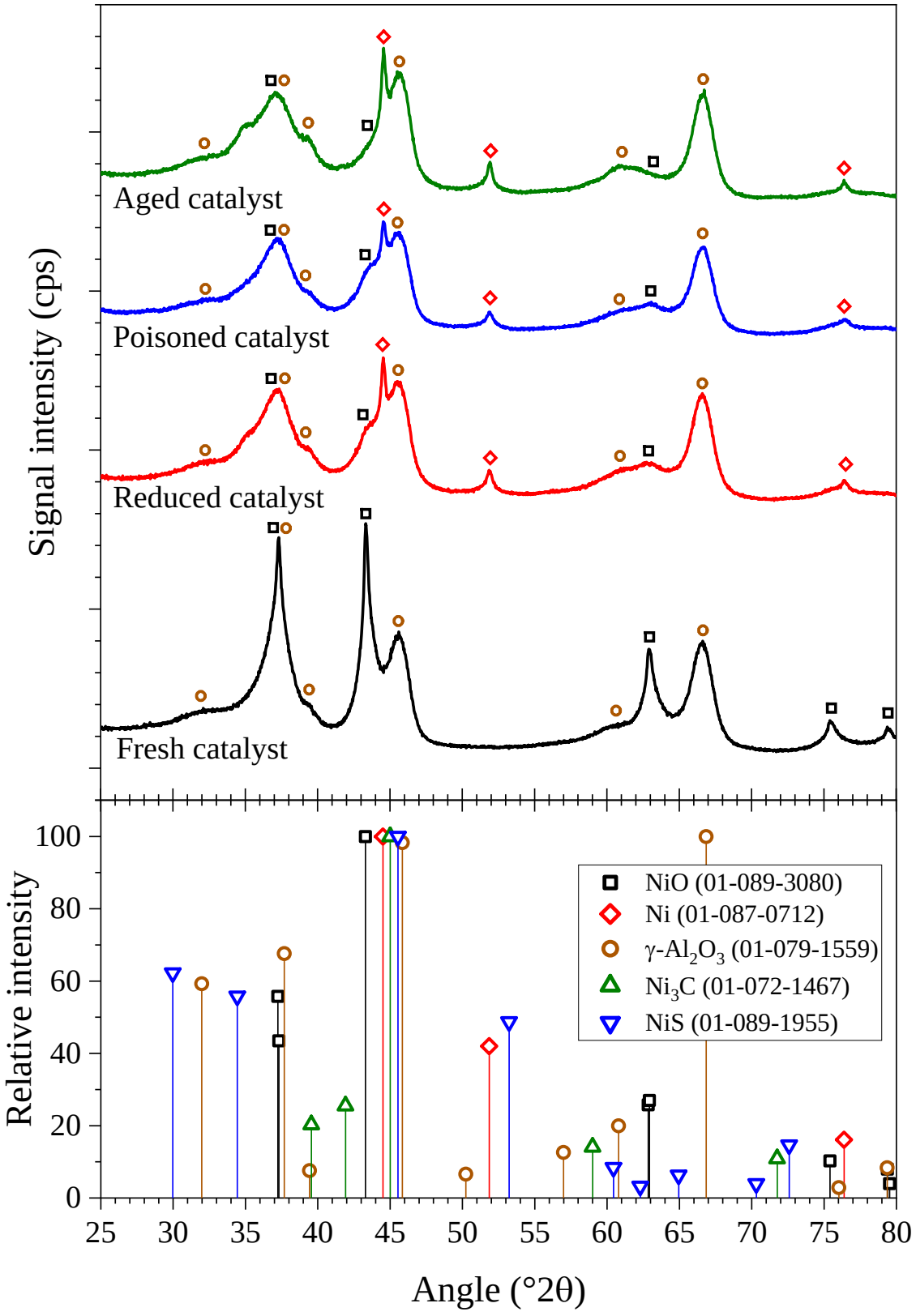

Figure S6. XRD measurements on the fresh, reduced, H_2S-poisoned and spent (under S05 conditions) catalysts.

7.5. TEM measurements

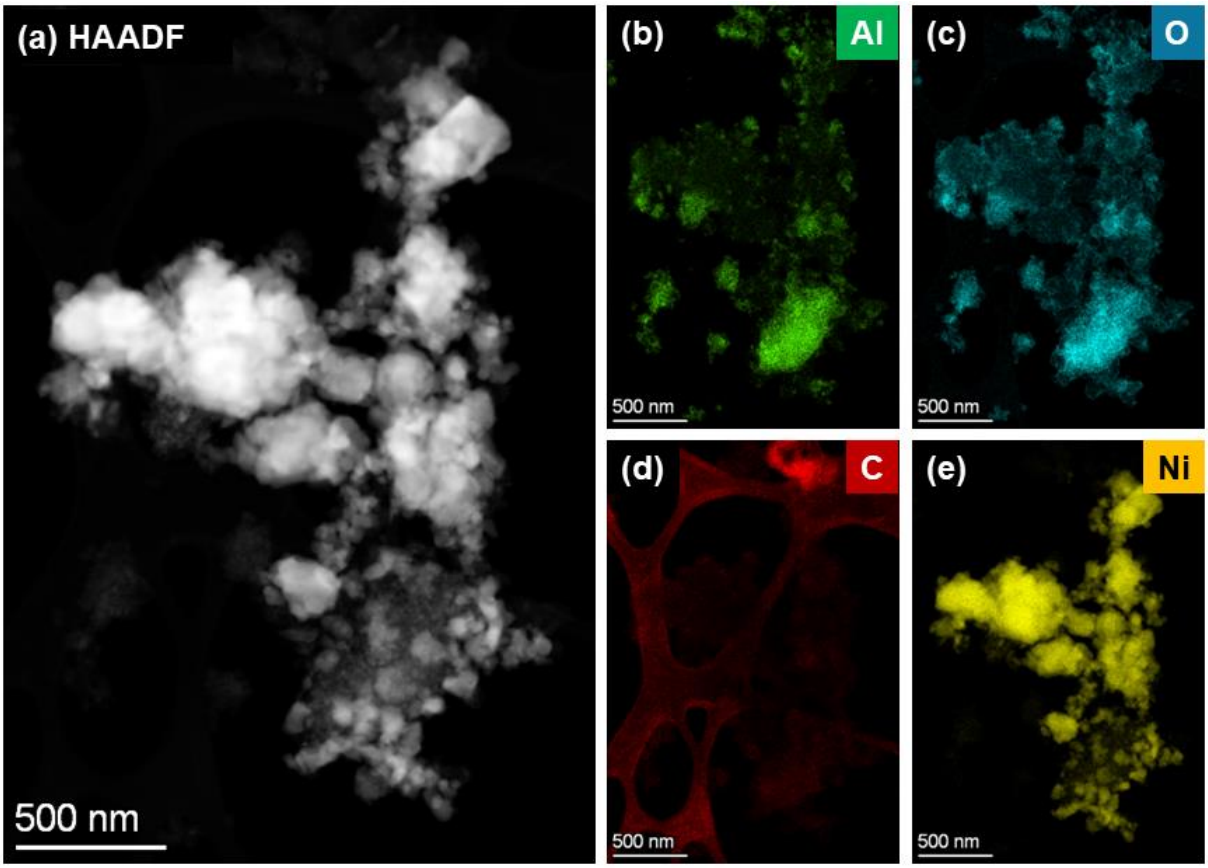

Figure S7. (a) HAADF-STEM and (b-e) EDS maps of an agglomerate of particles of the reduced catalyst (magnification: 33 kX).

8. Kinetic results

8.1. Effect of the volumetric flow rate

Figure S8 and Figure S9 show the influence of the residence time of the mixture as the volume flow rate changes for different temperatures. The equilibrium curves are also shown for CO_2 + H_2 tests. For CO methanation, the equilibrium is always close to 100 % of yield.

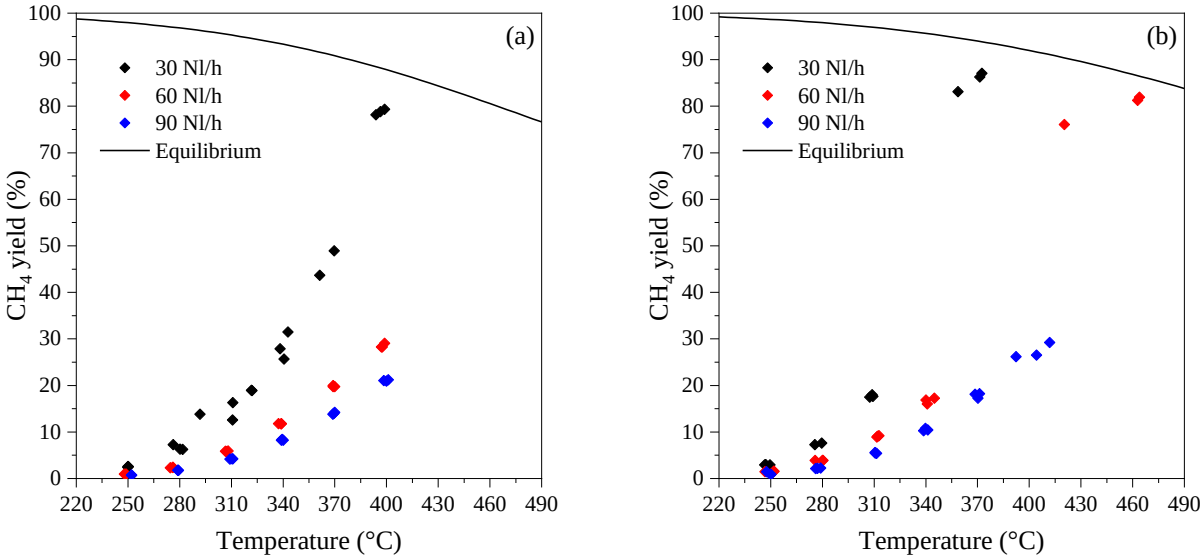

Figure S8. CH_4 yield with mixture $CO_2/H_2/N_2$ = 1/4/10 at 5 bar (a) and at 15 bar (b)

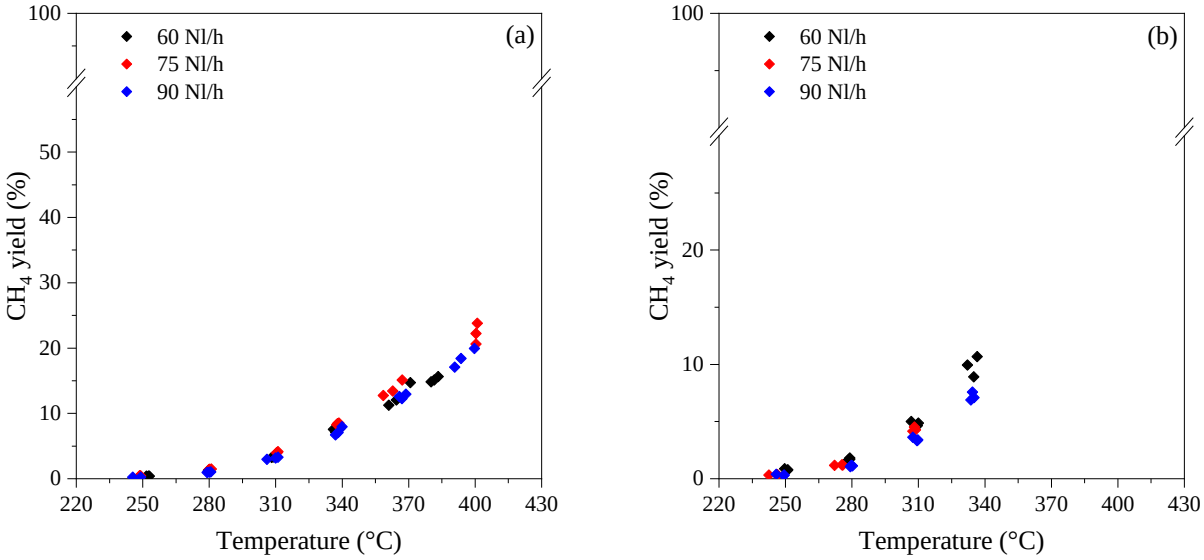

Figure S9. CH_4 yield with mixture $CO/H_2/N_2$ = 1/4/10 at 5 bar (a) and at 15 bar (b)

8.2. Effect of the CO_2 partial pressure

Figure S10 shows the influence of CO_2 partial pressure during CO_2 methanation. At 15 bar, at temperatures above 340 °C the system is brought to equilibrium conditions thus making thermal control complicated.

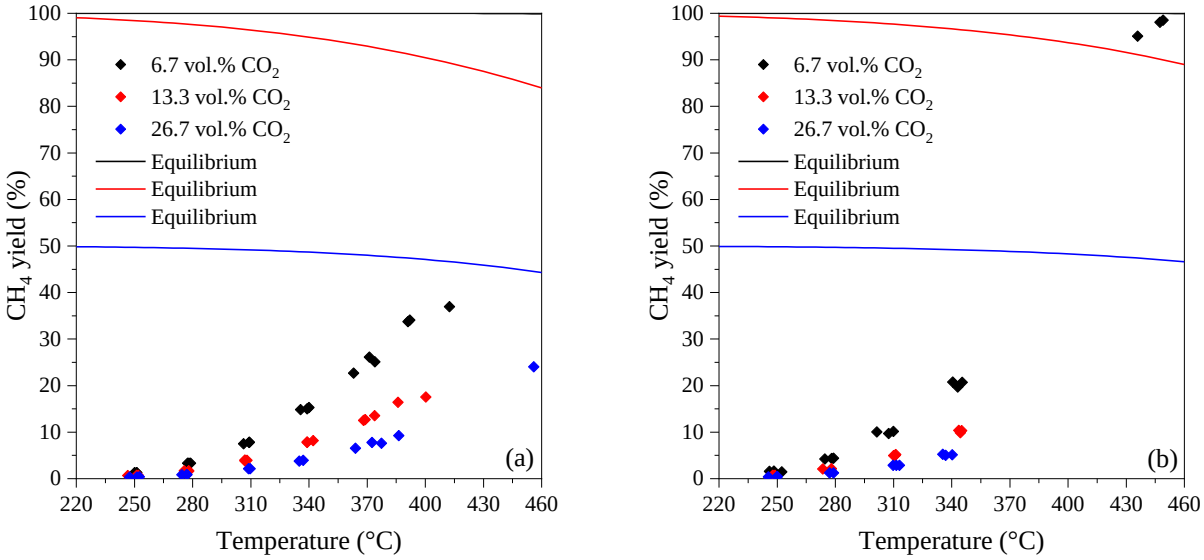

Figure S10. CH_4 yield with $CO_2/H_2/N_2$ gas mixture at 5 bar (a) and at 15 bar (b). Reaction conditions: gas flow rate 60 NL/h and H_2 molar fraction of 53.3 %.

8.3. Effect of the CO partial pressure

Figure S11 shows the influence of CO partial pressure. For these tests, the volumetric flow rate was increased to 90 Nl/h in order to decrease the residence time of the mixture and bring the system away from equilibrium conditions.

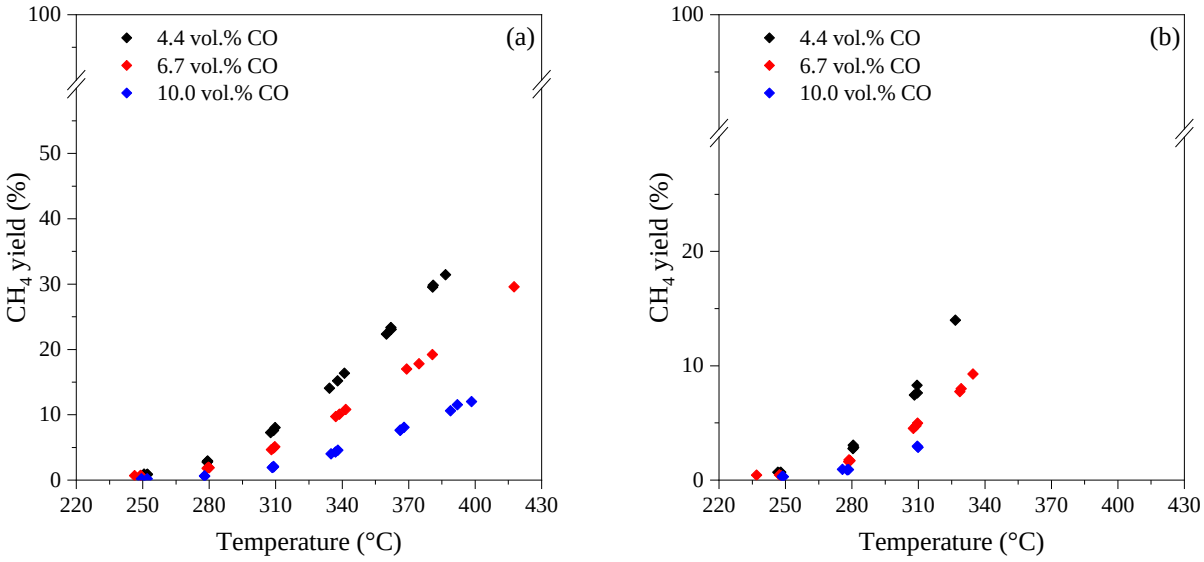

Figure S11. CH_4 yield with $CO/H_2/N_2$ gas mixture at 5 bar (a) and at 15 bar (b). Reaction conditions: gas flow rate 90 NL/h and H_2 molar fraction of 40.0 %.

8.4. Effect of the H_2 partial pressure

Figure S12 shows the influence of H_2 partial pressure for tests with CO_2 + H_2 reactant mixture while Figure S13 shows the influence of H_2 partial pressure for tests with CO + H_2.

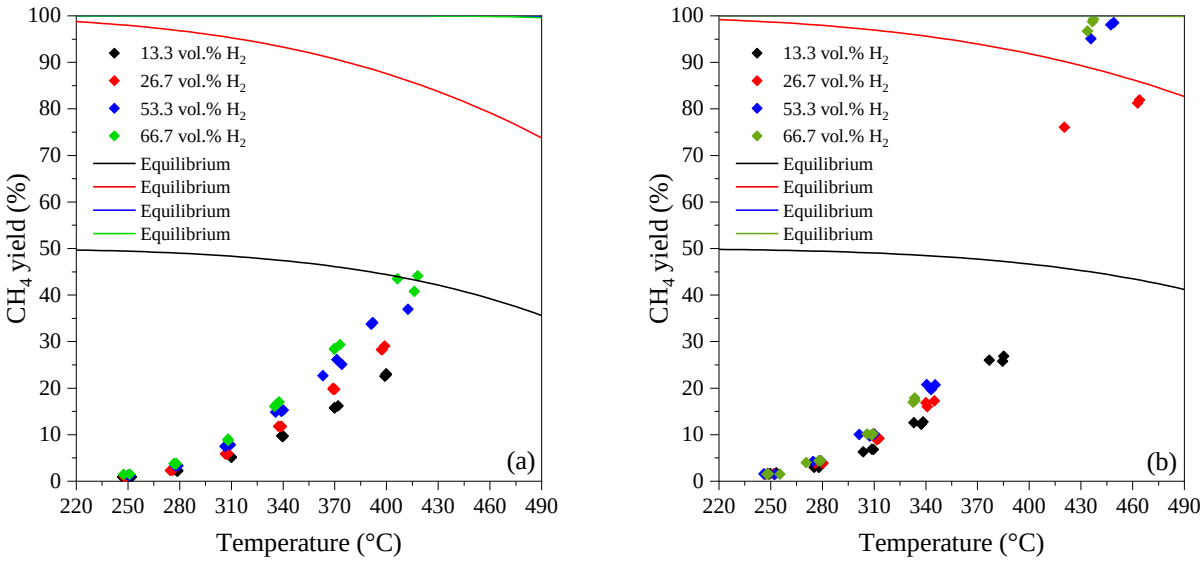

Figure S12. CH_4 yield with $CO_2/H_2/N_2$ gas mixture at 5 bar (a) and at 15 bar (b). Reaction conditions: gas flow rate 60 NL/h and CO_2 molar fraction of 6.7 %.

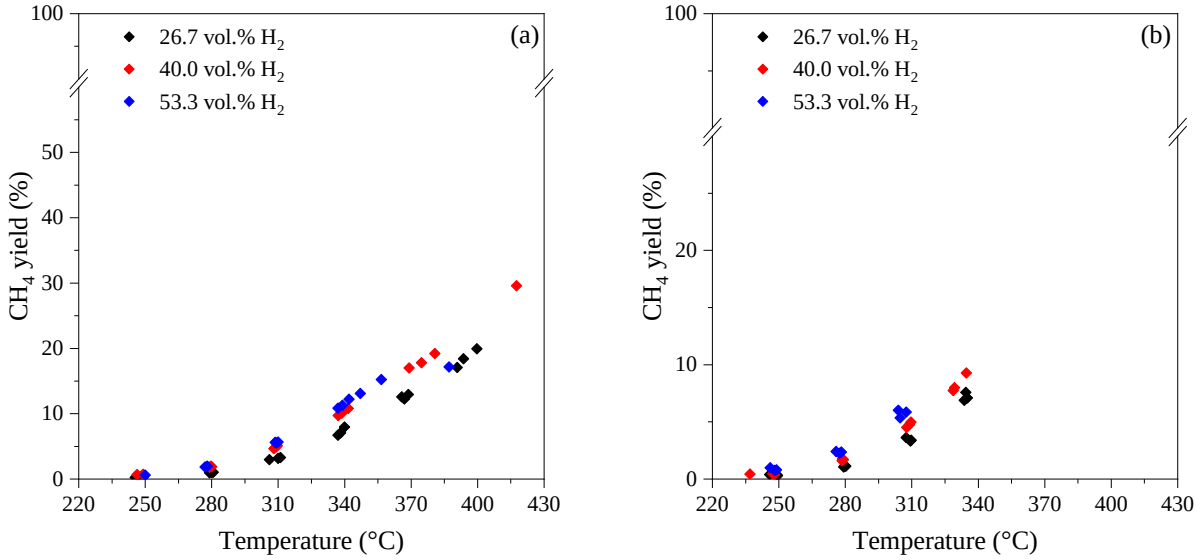

Figure S13. CH_4 yield with $CO/H_2/N_2$ gas mixture at 5 bar (a) and at 15 bar (b). Reaction conditions: gas flow rate 90 NL/h and CO molar fraction of 6.7 %.

9. Comparisons between model M3 and M4

A comparison of experimental and modeled CH_4 yield (models M3 and M4) is made in Figure S14.

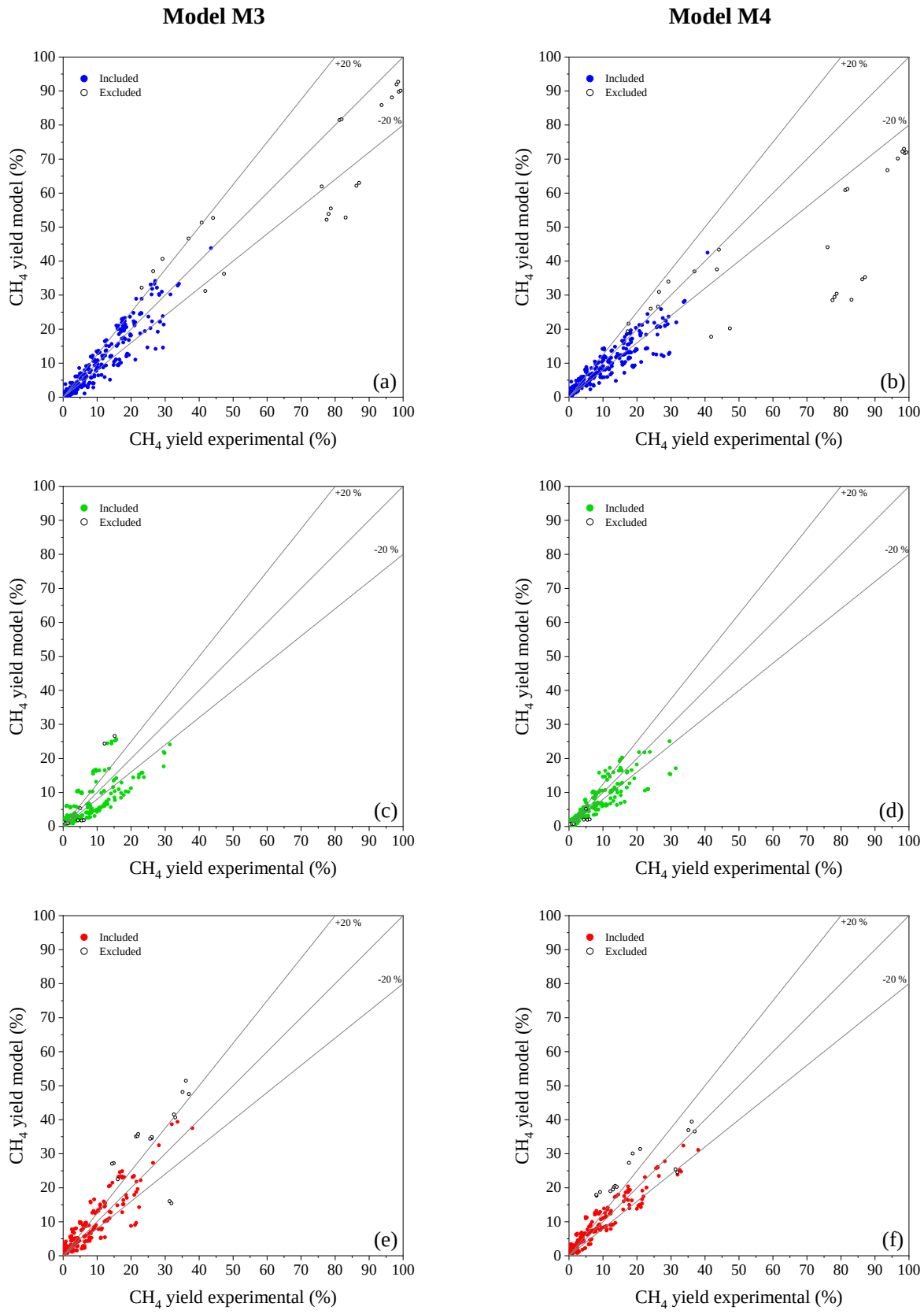

Figure S14. Parity plot comparing the experimental and modeled CH_4 yield for CO_2 dataset (a, b) CO dataset (c, d) and CO_2 + CO dataset (e, f).

The reliability and influence of the kinetic parameters was verified through a sensitivity analysis. Figure S15 illustrates the results of the sensitivity analysis conducted on the kinetic parameters of Model M4.

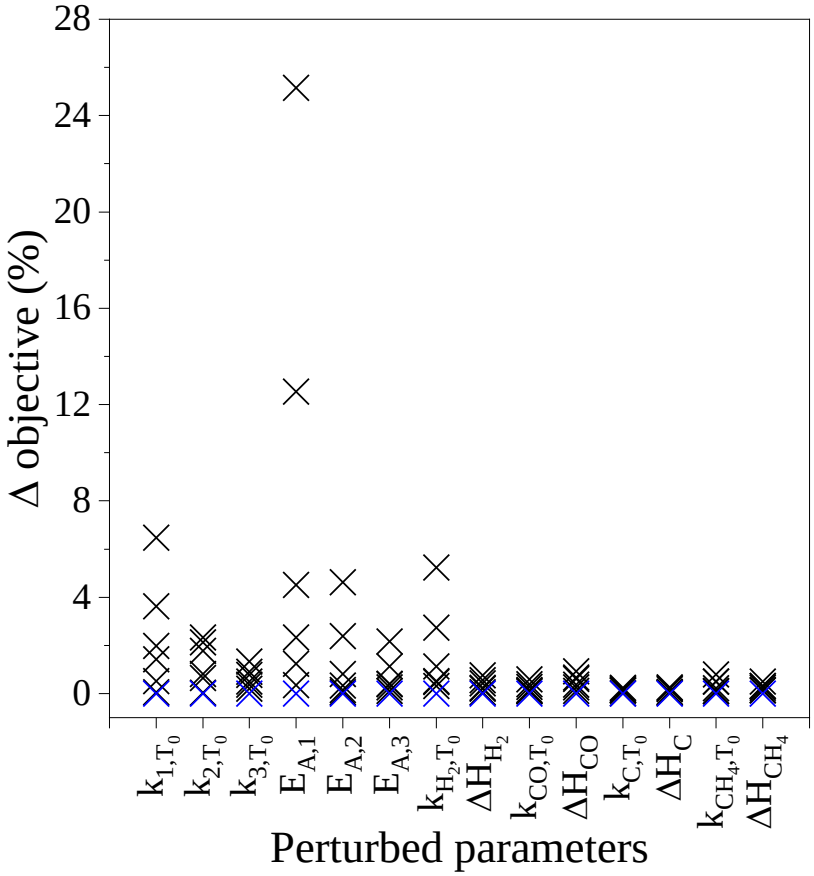

Figure S15. Parameters sensitivity analysis for kinetic model M4. The blue symbols represent the 0% variation and the black symbols represent ±10% variation steps. The range investigated is [-30%, +30%].

10. Stability and deactivation results

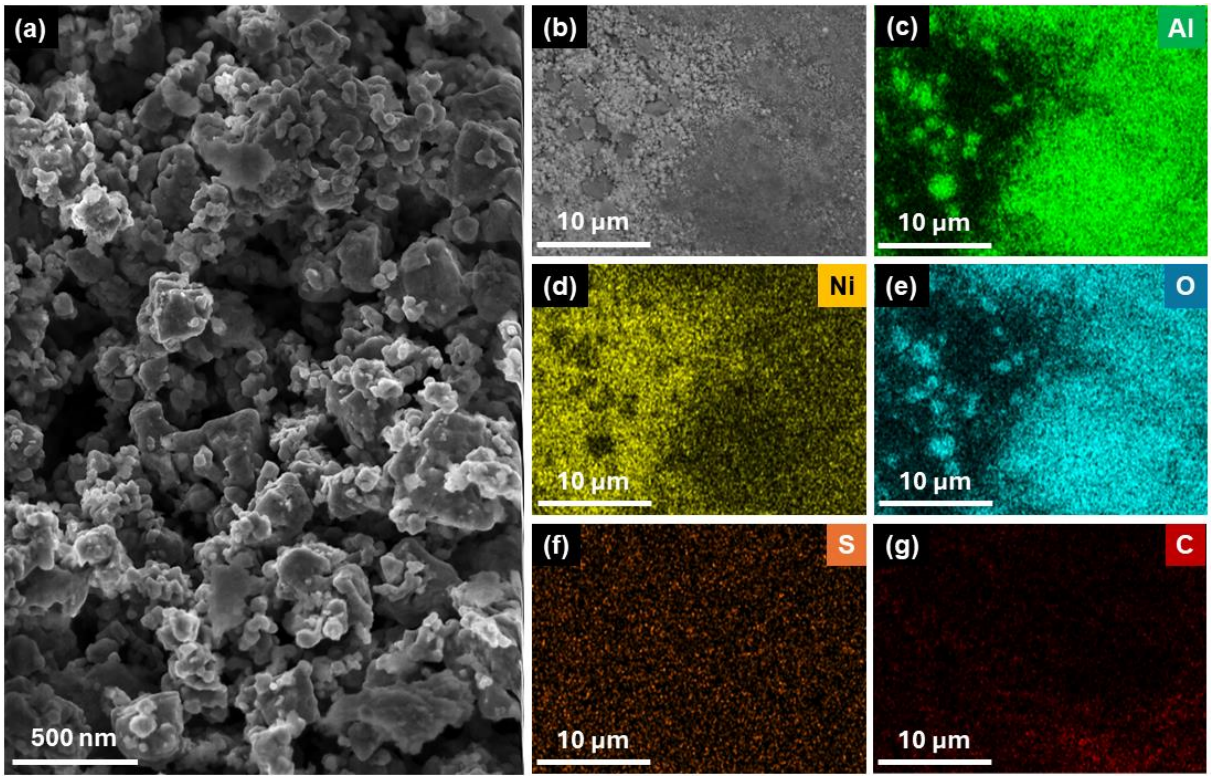

Figure S16. SEM-EDS images of the H_2S-poisoned catalyst at different magnifications: (a) 100 kX in SE mode, (b-g) 5 kX EDS map.

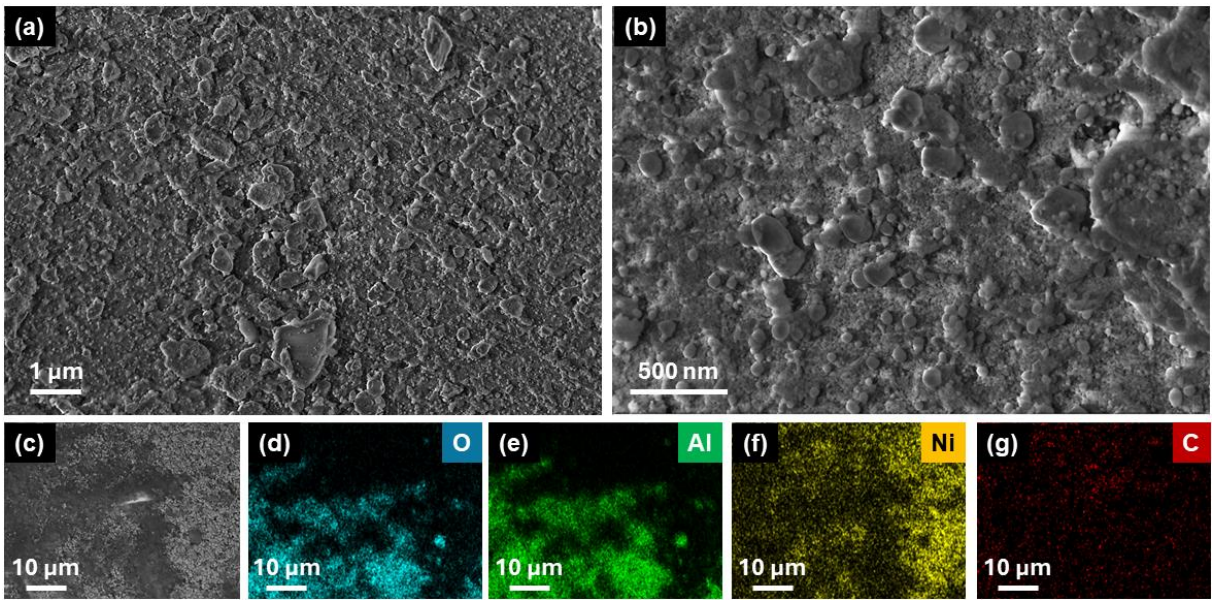

Figure S17. SEM-EDS images of the catalyst aged under S03 conditions (reaction temperature: 470 °C) at different magnifications: (a) 25 kX in SE mode, (b) 100 kX in SE mode, (c-g) 5 kX EDS map.

Higher selectivity toward hydrocarbons in the C_2-C_5 range was observed at low temperature (330 °C), while at higher temperature (425 °C) the selectivity towards light hydrocarbons decreases. Figure S18 shows the GC FID signal as a function of the retention time, identifying the different hydrocarbons species.

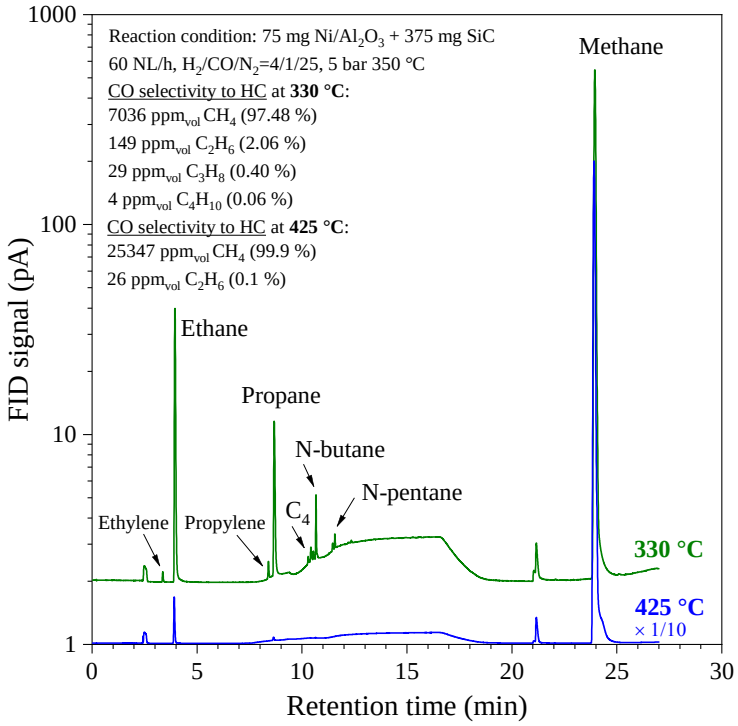

Figure S18. Differences in selectivity to hydrocarbons with H_2/CO ratio = 4 at 330 °C and 425 °C.

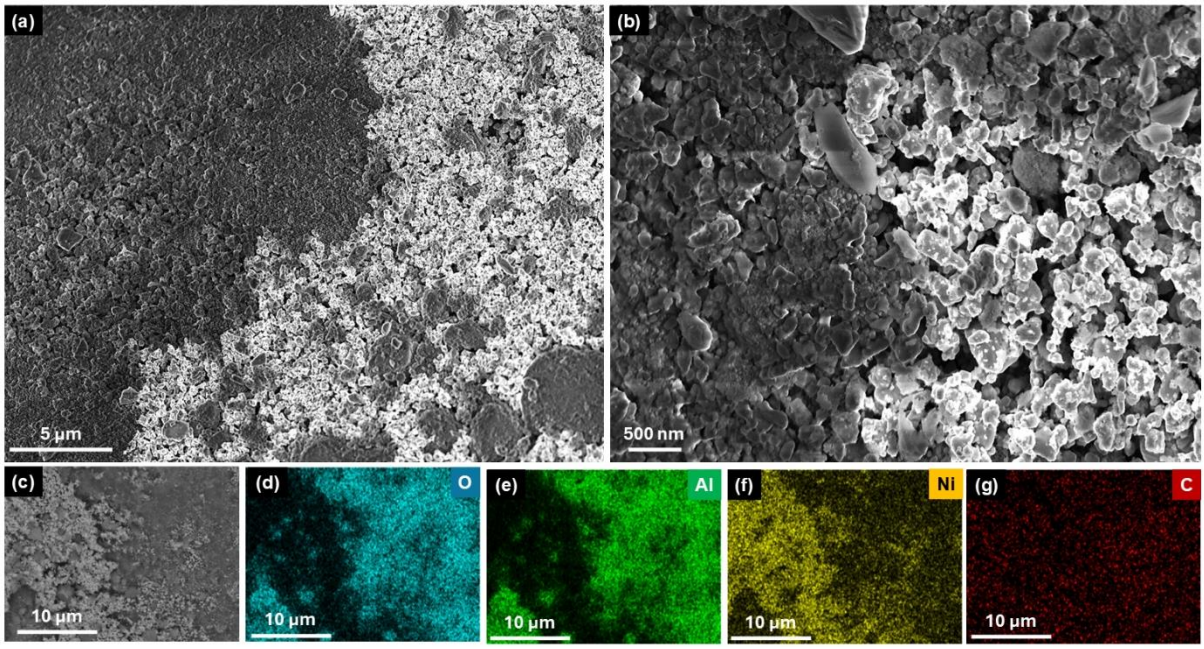

Figure S19. SEM-EDS images of the catalyst aged under S05 conditions at different magnifications: (a) 10 kX and (b) 100 kX in SE mode, (c-g) 10 kX EDS map.

Catalytic activity as a function of time on stream is shown in Figure S20. All deactivation tests were considered.

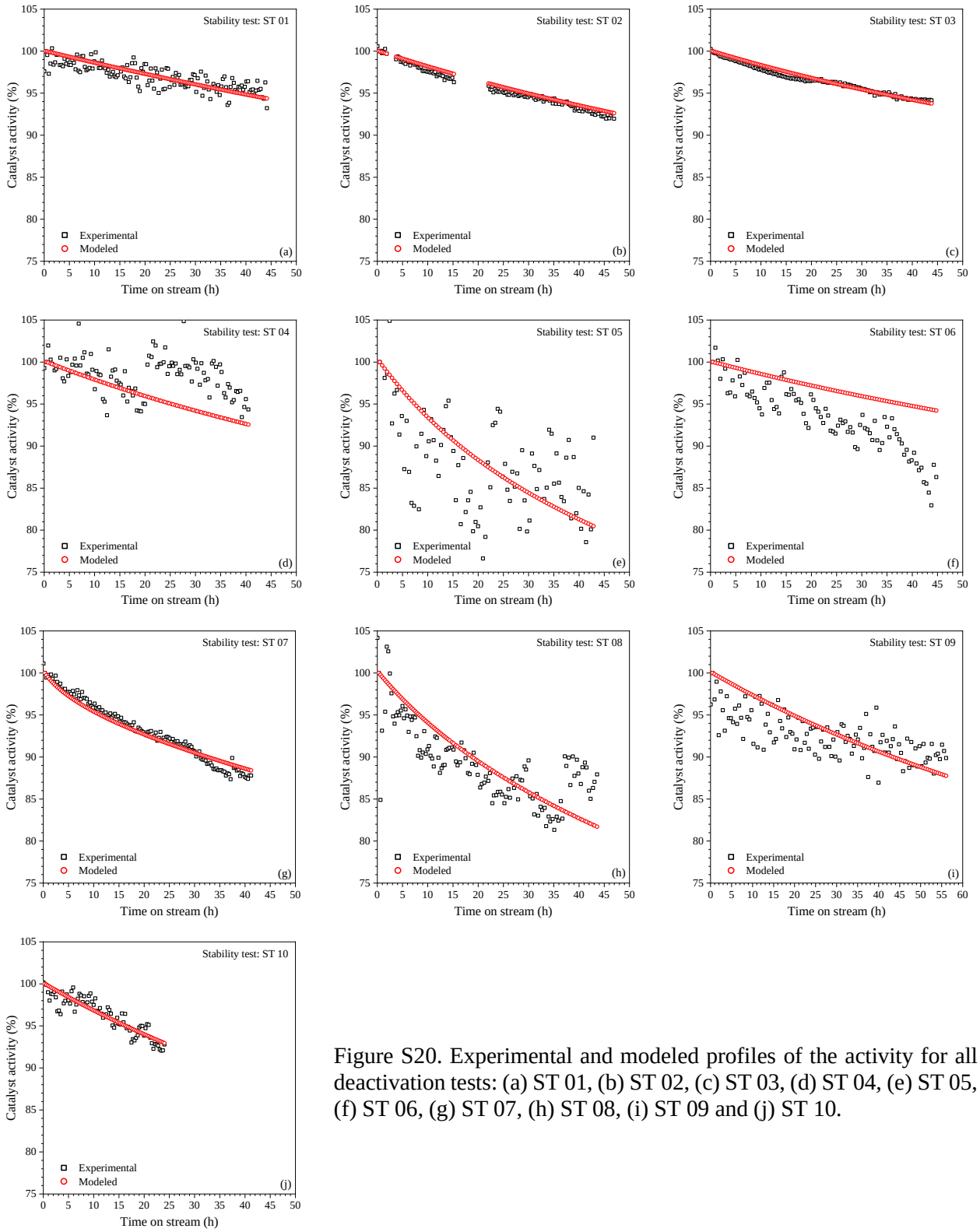

Figure S20. Experimental and modeled profiles of the activity for all deactivation tests: (a) ST 01, (b) ST 02, (c) ST 03, (d) ST 04, (e) ST 05, (f) ST 06, (g) ST 07, (h) ST 08, (i) ST 09 and (j) ST 10.

11. References

[1] NIST Chemistry WebBook, (n.d.). https://webbook.nist.gov/chemistry/ (accessed October 24, 2024).

[2] B.E. Poling, J.M. Prausnitz, J.P. O'Connell, The Properties of gases and liquids, 5th ed., McGraw-Hill, Inc., 2000.

[3] B. Todd, J.B. Young, Thermodynamic and transport properties of gases for use in solid oxide fuel cell modelling, J Power Sources 110 (2002) 186–200. https://doi.org/10.1016/S0378-7753(02)00277-X.

[4] R.H. Perry, D.W. Green, J.O. Maloney, Perry's Chemical Engineers' Handbook 9th edition, 9th ed, The McGraw-Hill Companies, 2019.

[5] B.R. Bird, W.E. Stewart, E.N. Lightfoot, Transport Phenomena, 2nd ed, John Wiley & Sons, New York, 2002. https://doi.org/10.1007/s007690000247.

[6] F. Koschany, D. Schlereth, O. Hinrichsen, On the kinetics of the methanation of carbon dioxide on coprecipitated $NiAl(O)_x$, Appl Catal B 181 (2016) 504–516. https://doi.org/10.1016/j.apcatb.2015.07.026.

[7] A. Quindimil, J.A. Onrubia-Calvo, A. Davó-Quiñonero, A. Bermejo-López, E. Bailón-García, B. Pereda-Ayo, D. Lozano-Castelló, J.A. González-Marcos, A. Bueno-López, J.R. González-Velasco, Intrinsic kinetics of CO_2 methanation on low-loaded Ni/Al_2O_3 catalyst: Mechanism, model discrimination and parameter estimation, Journal of CO_2 Utilization 57 (2022) 101888. https://doi.org/10.1016/j.jcou.2022.101888.

[8] E.A. Morosanu, F. Salomone, R. Pirone, S. Bensaid, Insights on a Methanation Catalyst Aging Process: Aging Characterization and Kinetic Study, Catalysts 10 (2020) 283. https://doi.org/10.3390/catal10030283.